

Accepted Manuscript

Benzothiazole carbamates and amides as antiproliferative species

Milica Videnović, Marija Mojsin, Milena Stevanović, Igor Opsenica, Tatjana Srdić-Rajić, Bogdan Šolaja



PII: S0223-5234(18)30739-6

DOI: [10.1016/j.ejmech.2018.08.067](https://doi.org/10.1016/j.ejmech.2018.08.067)

Reference: EJMECH 10678

To appear in: *European Journal of Medicinal Chemistry*

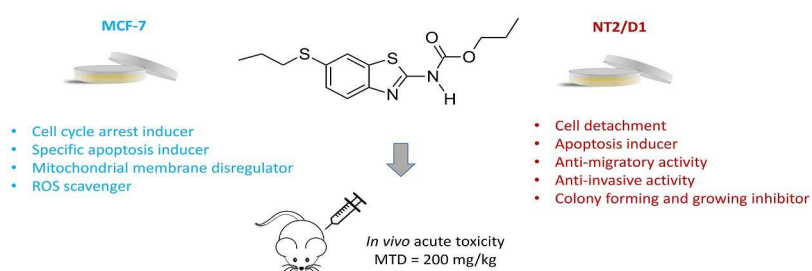
Received Date: 2 July 2018

Revised Date: 17 August 2018

Accepted Date: 25 August 2018

Please cite this article as: M. Videnović, M. Mojsin, M. Stevanović, I. Opsenica, T. Srdić-Rajić, B. Šolaja, Benzothiazole carbamates and amides as antiproliferative species, *European Journal of Medicinal Chemistry* (2018), doi: 10.1016/j.ejmech.2018.08.067.

This is a PDF file of an unedited manuscript that has been accepted for publication. As a service to our customers we are providing this early version of the manuscript. The manuscript will undergo copyediting, typesetting, and review of the resulting proof before it is published in its final form. Please note that during the production process errors may be discovered which could affect the content, and all legal disclaimers that apply to the journal pertain.



ACCEPTED MANUSCRIPT

Milica Videnović,[‡] Marija Mojsin,[¶] Milena Stevanović,^{¶,§,#} Igor Opsenica,[◇] Tatjana Srdić-Rajić,^{⊥,*} Bogdan Šolaja^{◇,#,*}

[‡]Faculty of Chemistry Innovative Centre, Studentski trg 12-16, 11158 Belgrade, Serbia

[¶]Institute of Molecular Genetics and Genetic Engineering, University of Belgrade, Vojvode Stepe 444a, 11010 Belgrade, Serbia

[§]University of Belgrade – Faculty of Biology, Studentski trg 16, 11158 Belgrade, Serbia

[#]Serbian Academy of Sciences and Arts, Knez Mihailova 35, 11158 Belgrade, Serbia

[◇]University of Belgrade – Faculty of Chemistry, Studentski trg 16, P.O. Box 51, 11158 Belgrade, Serbia

[⊥]Institute for Oncology and Radiology of Serbia, Pasterova 14, 11000 Belgrade, Serbia

Abstract

A series of new benzothiazole-based carbamates and amides were synthesized and their antiproliferative activity was determined. Derivatives with profound activity were identified and further investigated for their possible mechanism of action. It was found that these compounds induce specific apoptosis, G2/M cell cycle arrest and decrease ROS level in MCF-7 human breast cancer cell line. Moreover, submicromolar antiproliferative activity of examined carbamates against NT2/D1 testicular embryonal carcinoma was shown. The most potent derivatives strongly inhibited NT2/D1 cell migration and invasiveness.

Keywords: benzothiazoles, antiproliferative, MCF-7, NT2/D1, anoikis

1. Introduction

Cancer is a complex and lethal disease, responsible for more than 8 million deaths p.a. according to the World Health Organization report.¹ One of the main features of tumor cells is their rapid proliferation, and respective diversity.² Therefore, the discovery of new drugs that

would prevent the cell proliferation and induce apoptosis, stop cancer cell mobility and metastasis, is a long standing task of researchers in the field.

Benzothiazoles^{3,4} are prominent class of compounds that exert various pharmacological activities, such as antimicrobial,⁵ topoisomerase inhibitory activity,⁶ anti-HIV,⁷ multifunctional anti-Alzheimer's disease activity,⁸ anti-inflammatory activity,⁹ immunosuppressive (**1**, Frentizole),¹⁰ anticonvulsive and neuroprotective (**2**, Riluzole).¹¹ Members of benzothiazole chemotype are also potent anti-infectives – specifically possessing antimalarial^{12,13,14} and antileishmanial activity^{15,16} (compounds **3** and **4**, Figure 1). Benzothiazoles were investigated on several instances for their anti-cancer activity.¹⁷⁻²⁶ They were tested against selected number of cell lines, e.g., human cervical cancer, liver cancer, NSCL, prostate cancer, and human breast cancer exhibiting good to excellent antiproliferative activity with low toxicity. Former clinical candidate, Phortress (**6**), lysylamide prodrug of C(2) and C(6) substituted benzothiazole 5F203 (**5**), Figure 1) generates DNA adducts in sensitive cancer cell lines, including MCF-7 breast cancer cell line.¹⁷

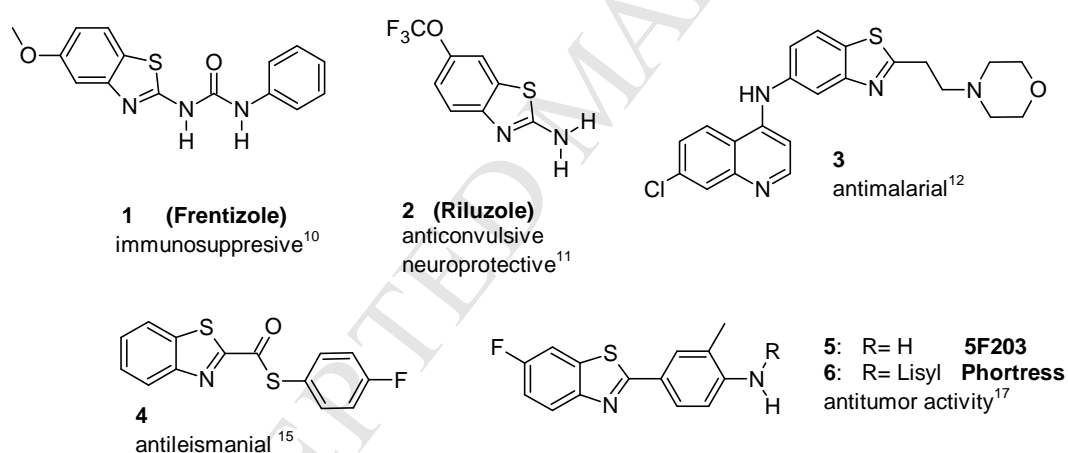


Figure 1. Sample structures of C(2) substituted benzothiazoles and their physiological properties.^{10,11,12,15,17}

In addition, the research on mechanism of action of individual benzothiazoles was the subject of few reports involving the induction of apoptosis by C(2)-substituted benzothiazolyl derivatives **7-10** (Figure 2).^{21,24,27,28}

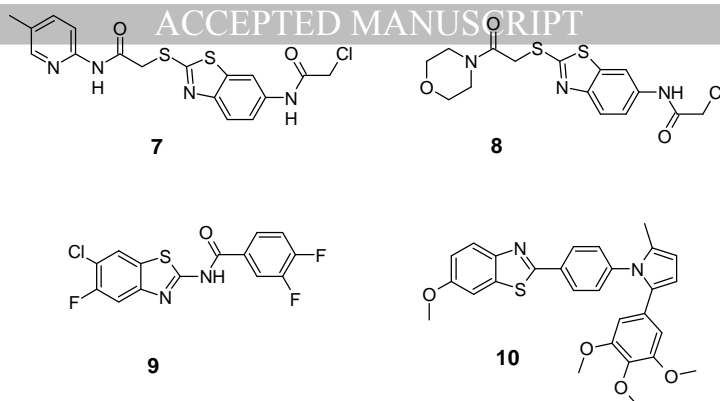


Figure 2. Benzothiazole chemotypes that induce apoptosis - compounds **7** and **8**: HepG2;^{21,27} compounds **9** and **10**: MCF-7.^{24,28}

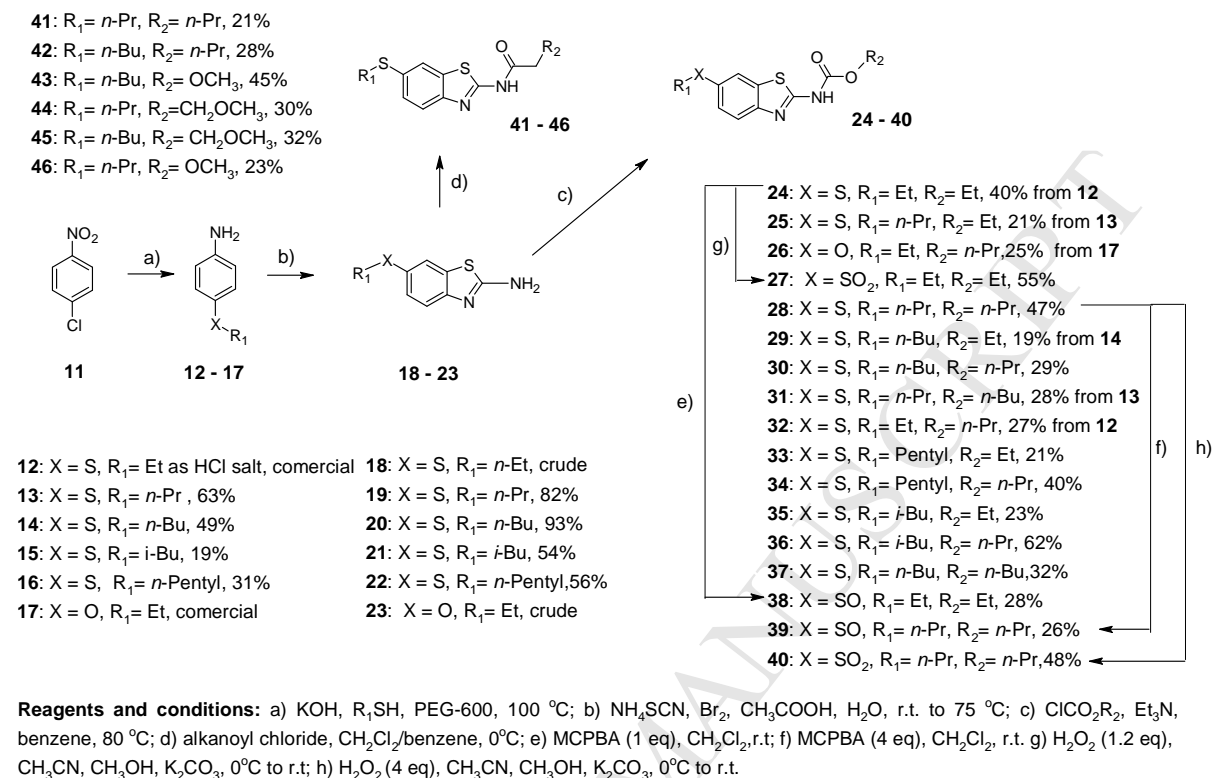
The above examples clearly indicate that substitution pattern at C(6) plays an important role in antiproliferative/anticancer activity of aminobenzothiazoles. We have chosen to introduce the thioalkyl substituent at C(6) in order to investigate the influence the electron-donor substituent (S) and respective electron-withdrawal (SO) and (SO₂) counterparts and explore the space around C(6) sulfur by changing the alkyl substituents while keeping the carbamate moiety at C(2) nitrogen. For comparison, we also prepared respective C(6) oxygen analogue, as well as few amides.

Therefore, we report the synthesis, activity and investigation on modes of action of new benzothiazole chemotype against breast cancer cell lines MCF-7 and testicular embryonal carcinoma NT2/D1. Furthermore, the newly synthesized benzothiazole-based carbamates were evaluated against NT2/D1 cells in terms of antimigratory activity. To the best of our knowledge, only a limited number of benzothiazole-based apoptosis inducers in MCF-7 human breast cancer cell line (compounds **9** and **10**, Figure 2) have been reported. Their proapoptotic activity was confirmed either by ELISA detection of mono- and oligonucleosomes enrichment after treatment,²⁸ or caspase-9 activity.²⁴ Moreover, there is no report of benzothiazole-based compounds with antiproliferative and antimigratory potential against NT2/D1 testicular teratocarcinoma cell line.

2. Chemistry

A series of novel benzothiazole carbamates and amides were synthesized starting with commercially available 1-chloro-4-nitrobenzene which was converted to 4-(alkylthio)anilines (**13** – **16**) by one-pot transformation in a reaction with the appropriate alkyl thiols and KOH in PEG-600 (Scheme 1).²⁹ Aminobenzothiazole moiety was obtained in reaction of 4-substituted anilines with NH₄SCN using bromine in acetic acid according to modified procedure for

synthesis of aminobenzothiazole core.³⁰ After submitting aminobenzothiazoles to further derivatization with different alkyl chloroformates, the target carbamate derivatives (**24** – **26** and **28** – **37**) were obtained in 19 – 62% yield.



Scheme 1. Synthesis of aminobenzothiazole derivatives.

Oxidation of sulfide **24** was achieved with one or four equivalents of MCPBA³¹ at room temperature in CH₂Cl₂ to obtain sulfoxo and sulfonyl derivatives **27** and **38**, respectively. To investigate the influence of antioxidant properties of our aminobenzothiazoles on ROS production, and further impact on antiproliferative activity against MCF-7 cancer cell line, we have also synthesized **39** and **40**, sulfoxo and sulfonyl analogues of carbamate **28**. For this transformation, H₂O₂ was used³² as MCPBA afforded only complex reaction mixture. The synthesis of benzothiazole-based amide derivatives (**41** – **46**) was performed under mild reaction conditions starting from amines **19** and **20** and synthesized alkanoyl or alkoxyalkanoyl chlorides.

3. Results

3.1. Biological evaluation

3.1.1. In vitro antiproliferative screening and cytotoxicity evaluation

Seventeen selected compounds (**24** – **38**, **41** and **44**) were submitted to NCI-60 Cell Screen through the Developmental Therapeutics Program (DTP) in National Cancer Institute (NCI).

Selected compounds were initially tested at a single dose (10 μ M) against the full NCI 60-cell panel (data not shown), following the accepted DTP protocol.³³ Seven benzothiazole carbamates (**24** – **26**, **28** – **30** and **33**) satisfied pre-determined inhibition threshold criteria in a minimum number of cell lines and were evaluated against the 60-cell panel at five concentrations level. Table 1 reveals mean GI₅₀ (μ M) values (MID) for selected compounds tested against full 60-cell panel after 48 h treatment obtained using SRB assay (full data are given in Supplementary material).

Table 1. Mean GI₅₀ (μ M) values (MID) for selected compounds obtained after 48 h treatment against a panel of 60 cell lines in vitro ^a

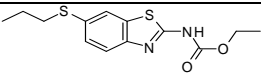
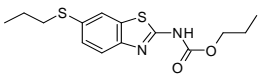
Compound	24	25	26	28	29	30	33
MID ^b	19.9	2.13	81.2	2.14	0.74	0.58	0.83

^a Five dose assay was performed against 60 cancer cell lines treated with selected compounds for 48 hours using SRB procedure

^bMID = Mean GI₅₀ values for each compound against full 60-cell panel

The most potent compound was **30** with GI₅₀ values in submicromolar range against the majority cell lines of 60-cell panel, followed by compounds **29** and **33**. Considering investigated ethyl carbamates (**24**, **25**, **29** and **33**), lengthening of the alkyl group linked to S-C(6) attached to benzothiazole moiety led to enhanced antiproliferative activity according to MID (submicromolar MID GI₅₀ values for butyl and pentyl derivatives **29** and **33** vs. MID GI₅₀ > 2 μ M for ethyl and propyl derivatives **24** and **25**). Compound **26**, containing O-C(6) substituent instead of S-C(6), with the highest GI₅₀ value (>80 μ M), clearly emphasized the importance of S-C(6) for the antiproliferative activity. Cytotoxic/antiproliferative activities of synthesized benzothiazole derivatives were further evaluated against four tumor cell lines (estrogen receptor positive breast adenocarcinoma MCF-7, myelogenous leukemia K562, melanoma A375, testicular embryonal carcinoma NT2/D1) and human lung fibroblast MRC-5 cell line derived from normal lung tissue. Standard MTT assay was applied after 48h cell exposure to the tested compounds (**25**, **26**, **28** – **30**, **32**, **34** – **37**, **39** – **46**) (Table 2 and Supplementary material I)

Table 2. IC₅₀ values calculated for selected compounds (**25**, **28** – **30**, **36**, **39** – **41**, **44**, **45**).^c

Compound	Structure	MCF-7 (IC ₅₀ , μ M)	A375 (IC ₅₀ , μ M)	K562 (IC ₅₀ , μ M)	NT2/D1 (IC ₅₀ , μ M)	MRC-5 (IC ₅₀ , μ M)
25		61.4 \pm 4.2	85.0 \pm 5.6	> 100	>1	-
28		24.2\pm3.1	> 100	> 100	0.2\pm0.03	> 300

29		> 100	91.6±6.0	> 100	>1	-
30		> 100	45.2±3.4	> 100	0.1±0.01	>300
36		> 100	> 100	7.7±2.0	>1	-
39		> 100	-	-	-	-
40		> 100	-	-	-	-
41		30.5±2.5	77.5±4.5	53.2±4.0	>1	> 300
44		95.5±5.5	> 100	66.3±4.2	>1	-
45		92.5±5.0	> 100	44.2±3.3	>1	-
Doxorubicin		0.4	-	2	-	-
Cisplatin		-	-	-	1.11±0.17	-

^cIC₅₀ values were calculated after 48 h treatment of selected cell lines with five concentrations of investigated compounds using MTT assay. The measurements were performed in triplicate.

Obtained results indicated a high sensitivity of NT2/D1 cell line towards carbamates **28** and **30** with IC₅₀ values 0.2 and 0.1 μM, respectively. The activity of both inhibitors against NT2/D1 was investigated in detail, vide infra.

The MTT assay indicated that other tumor cell lines (K562, A375 and MCF-7) mostly keep their metabolic activity after 48 h exposure to examined compounds. Notable IC₅₀ values (24.2 μM and 30.5 μM) were estimated for carbamate **28** and amide **41** (R₁ = R₂ = n-Pr) against MCF-7 cells, while compound **41** was also active against A375 and K562 cells. Additional methylene group in alkylthio chain induced a complete lack of activity for compound **42** (Supplementary material). The most active compound against K562 cell line was iso-butyl derivative **36** with IC₅₀ = 7.7 μM.

High IC₅₀ values (>300 μM) for compounds **28**, **30**, and **41** against control MRC-5 line, indicated good selectivity of benzothiazole derivatives for cancer cell lines and very low toxicity against normal human cell line in vitro.

Our newly synthesized aminobenzothiazole derivatives with the observed antiproliferative activity were investigated for their mechanism of action. We have chosen two cancer cell lines, moderately sensitive MCF-7 and very sensitive NT2/D1 cells. First we tested the molecular mechanisms underlying the inhibitory effect of carbamate **28** and amide **41** on the proliferation and viability of MCF-7 cells.

3.1.2. Treatment of MCF-7 cells with benzothiazole derivatives induced G2/M arrest and increased expression of cyclin B1

To investigate possible antiproliferative effects we selected IC₅₀ concentration for compounds **28** and **41** and analyze their effects on cell cycle distribution of MCF-7 at two time points (24 and 48 h treatments). Applied equipotent concentrations were 25 μ M for **28** and 30 μ M for **41**. Treatment with these compounds exhibited time-dependent effects on MCF-7 cell cycle progression. Both examined compounds induced the accumulation of cells in G2/M phase after 24 h treatment. It is followed by gradual increase in apoptotic cell population (sub-G1 phase) with reduction of cells in both G0/G1 and S cell cycle phases compared to untreated control cells (Figure 3). Extended 48 h treatment of MCF-7 cells (Figure 4) resulted in further increase in cell death (sub-G1 phase cells around 50%).

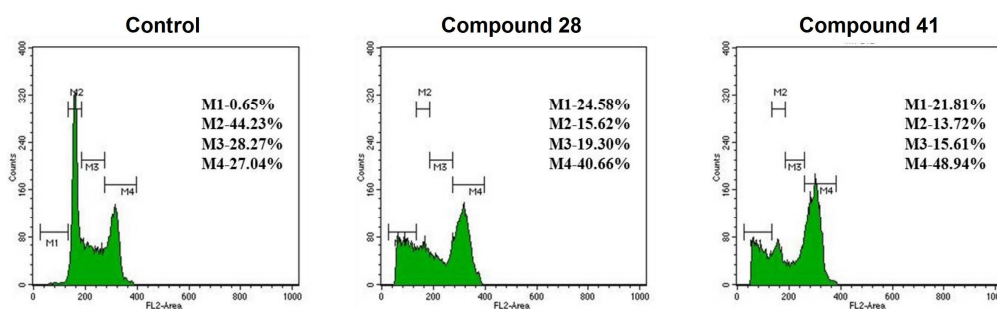


Figure 3. Cell cycle distribution after 24 h treatment (M1 – sub G1, M2 – G0/G1, M3 – S, M4 – G2/M).

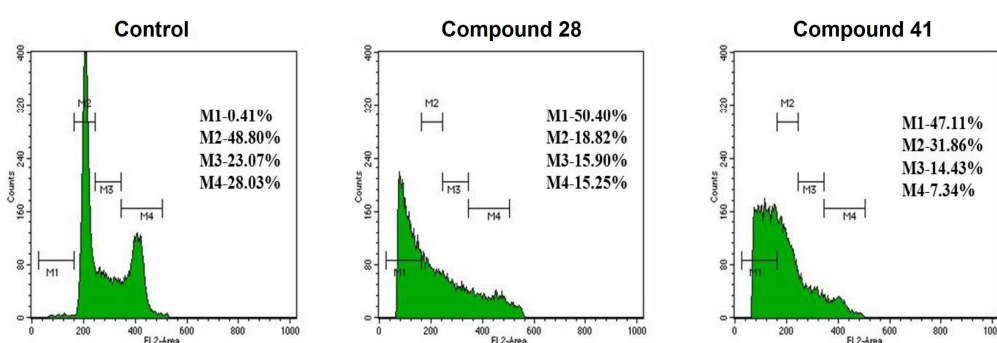


Figure 4. Cell cycle distribution after 48 h treatment (M1 – sub G1, M2 – G0/G1, M3 – S, M4 – G2/M)

To gain insight into events preceding G2/M arrest of MCF-7 cells, we measured the expression of cyclin B1, one of the regulatory proteins that control mitosis, during 24 h treatment with the already applied concentrations of tested compounds. Flow cytometric

analysis revealed that treatment of MCF-7 cells induced the increase in cyclin B1 expression (Figure 5), what is in accordance with accumulation of cells in G2/M phase after 24 h.

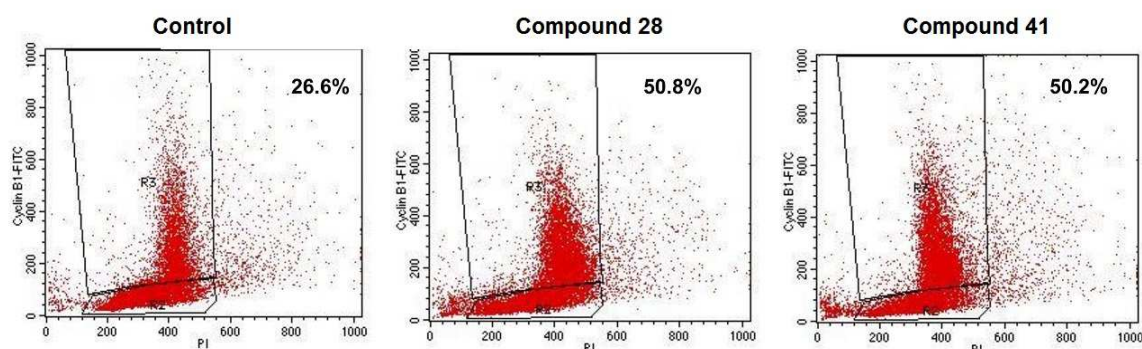


Figure 5. Level of intracellular cyclin B1 after 24 h treatment of MCF-7 cells with antiproliferatives **28** and **41**

3.1.3. Translocation of cell membrane phosphatidyl serine

The observed apoptosis-inducing effect of investigated compounds was also confirmed by bivariate Annexin V-FITC/PI flow cytometry. We examined the kinetics of induced apoptosis at IC_{50} concentrations of compounds **28** and **41**. In line with previous results, 24 h and 48 h treatments induced significant increase in programmed cell death (Figure 6). Apoptosis effects were time dependent with the highest number of early apoptotic MCF-7 cells detected 48 h after the treatment (61% and 49% for compounds **28** and **41**, respectively). In addition, low level of late apoptotic/necrotic cells was observed.

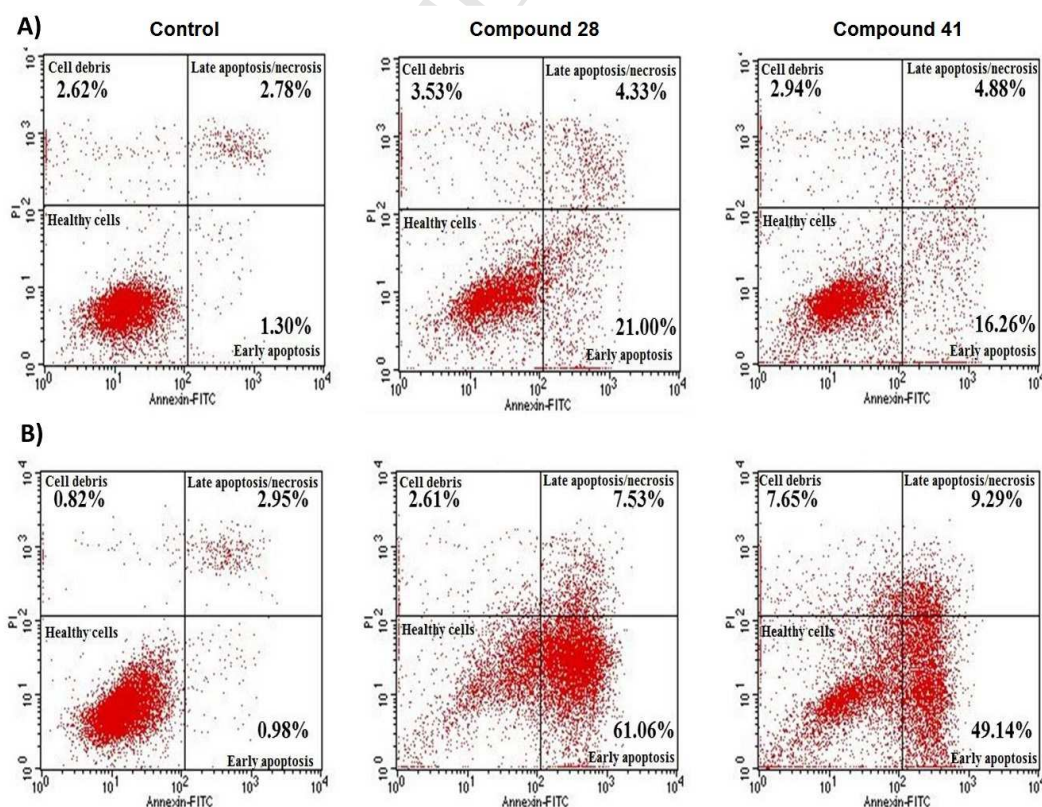


Figure 6. Effects of compounds **28** and **41** on apoptosis in terms of Annexin-V and PI staining of MCF-7 cells for 24 h (A) and 48 h (B).

3.1.4. Benzothiazole derivatives induced mitochondrial events related to apoptosis in MCF-7 cells

Data obtained by measuring the translocation of the cell membrane phosphatidyl serine revealed the increased population of early apoptotic MCF-7 cells upon treatment with compounds **28** and **41** (Figure 6). Consequently, we examined the observed pro-apoptotic effects of tested compounds in relation to mitochondrial injury. We performed FACS Rh123 fluorochrome incorporation assay.³⁴ The mitochondrial membrane potential ($\Delta\Psi_m$) changed slightly after 24 h of MCF-7 cell treatment with both investigated compounds (Figure 7A). In contrast, a significant loss of $\Delta\Psi_m$ in more than 80% MCF-7 cells, was observed upon 48 h treatment (Figure 7B) indicating that apoptosis induced by **28** and **41** involved mitochondrial dysregulation.

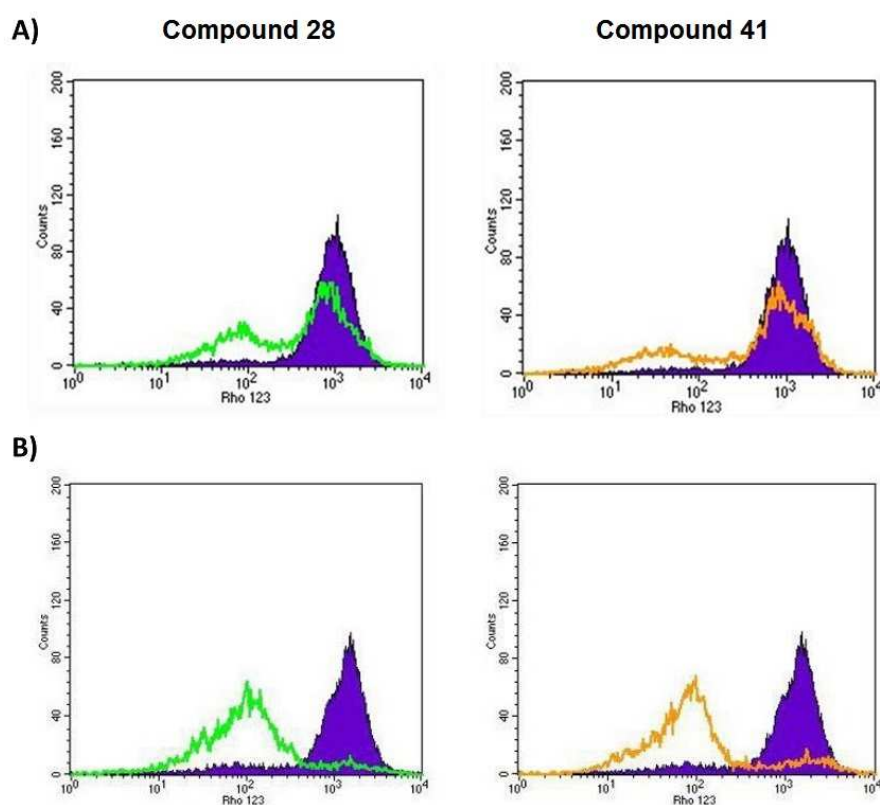


Figure 7. Mitochondrial membrane potential (MMP) in MCF-7 cells after 24 h (A) and 48 h (B) treatment with **28** and **41** compared to control cells' MMP (violet)

The relative levels of pro-apoptotic proteins such as Bax and anti-apoptotic proteins such as Bcl-2 determines whether cell death will occur following an apoptotic stimulus. The Bax/Bcl-2 complex regulates the mitochondrial membrane permeability.³⁵ The overexpression of the pro-apoptotic Bax induces the loss of the mitochondrial membrane potential that

initiates the progression of apoptosis. Considering dysregulation of mitochondrial membrane, we evaluated Bax/Bcl-2 ratio during the treatment of MCF-7 cells with compounds **28** and **41** at single equipotent concentration 24 and 48 h after treatments. FACS analysis performed to quantify the pattern of Bax and Bcl-2 expressions revealed that incubation with tested compounds for 24 h resulted in increased protein expression of the mitochondrial pro-apoptotic protein Bax (Figure 8). On the other hand, exposure to these agents for 24 h did not significantly modify the expression of Bcl-2. This resulted in slightly increased Bax/Bcl-2 ratio (Figure 8). After 48 h of treatment, protein expression of Bax increased further, while expression of Bcl-2 decreased, which resulted in significant increase of Bax/Bcl-2 ratio and the observed apoptosis (Figure 8). Derivative **28** exhibited more than 5-fold increase of Bax/Bcl-2 ratio compared to untreated cells after 48 h treatment.

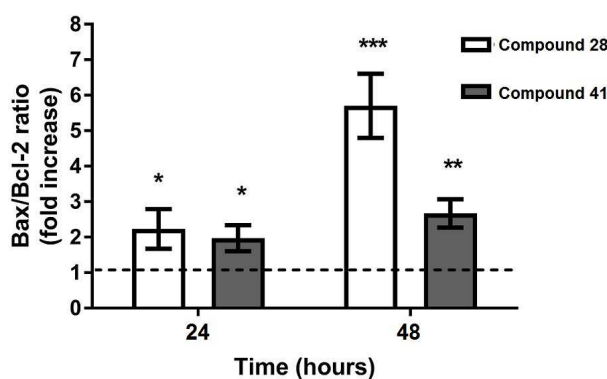


Figure 8. Bax/Bcl-2 ratio (fold increase compared to control cells) after 24 and 48 h treatment of MCF-7 cells with tested benzothiazoles at IC_{50} concentration. * $P < 0.05$, ** $P < 0.01$, *** $P < 0.001$

To identify the putative involvements of p53 and p73 proteins in pro-apoptotic effect of benzothiazole derivatives, protein expressions were measured in treated cell line. The expression of p53 and p73 proteins was measured in MCF-7 cells treated with IC_{50} concentrations of **28** and **41** using flow cytometry at two time points. Twenty four hour treatment induced significant p53 protein accumulation and a persistently increased level was observed up to 48 h (Figure 9A), along with reduction of p73 expression level at both time points (Figure 9B), implicated that apoptosis induced by examined compounds might be mediated by p53-dependent pathway.

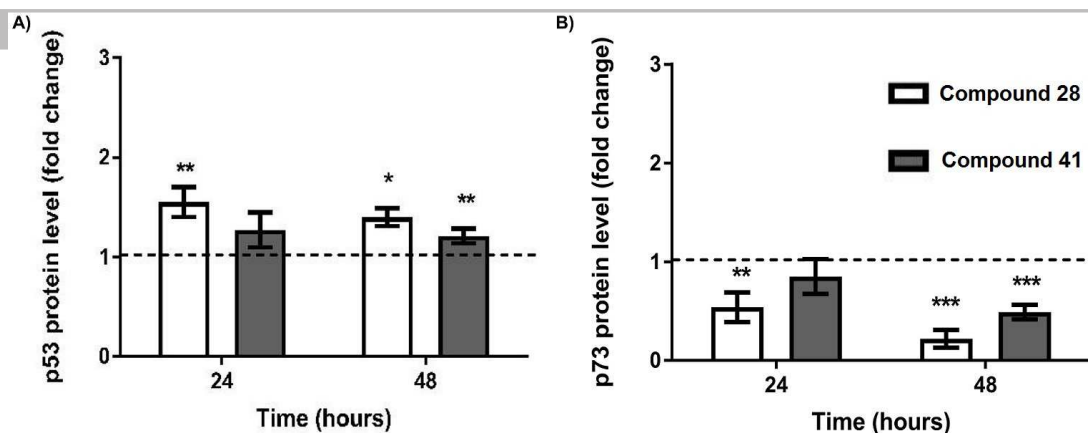


Figure 9. p53 (A) and p73 (B) protein level (fold change compared to control) in MCF-7 cells after benzothiazole treatment. *P < 0.05, **P < 0.01, ***P < 0.001

3.1.5. Benzothiazole derivatives sharply reduced reactive oxygen species (ROS) production in MCF-7 cell line

Affecting ROS production in tumor cells is one of therapeutic approaches for treating cancer. Based on the structures of investigated inhibitors with R₁S-C(6) possibly rendering antioxidant properties, we conducted experiments to check whether our compounds scavenge ROS and would that activity be related to their pro-apoptotic effect. The ROS level was measured in MCF-7 cells treated with compounds **28** (c = 25 μM) and **41** (c = 30 μM) for 24 and 48 h by flow cytometry using fluorescent dye DCFH-DA. The obtained data demonstrated that both compounds significantly decrease the ROS level in MCF-7 cells after 24 h treatment (Figure 10) with a persistent reduction of ROS production after 48 h treatment. In addition, we have tested the effects of sulfoxide and sulfonyl analogues of **28**, **39** and **40**, respectively, after 24 h treatment (c = 25 μM). Results demonstrated in Figure 11 show that these derivatives with higher oxidation state of sulfur exhibited reduction of ROS accumulation to a lesser extent, which can be ascribed to their reduced antioxidative ability. Partial ROS suppressing activity of sulfonyl derivative **40** indicated the possibility of thiazole sulfur's antioxidative properties. Along with this observation, the RO-C(6) derivative **26** was checked for its possible antioxidative action (c = 25 μM). This compound, containing only thiazole sulfur, induced 15% decrease in ROS accumulation compared to control cells after 24 h treatment (Figure 11), thus retaining the potential antioxidative properties. Taken together, these results showed that ROS affecting activity of examined benzothiazole derivatives is strongly enhanced with RS-C(6) substituent, however, the thiazole sulfur also contributes to overall antioxidative action.

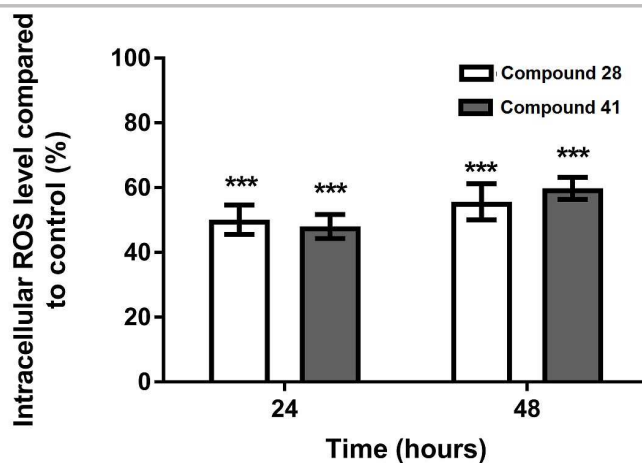


Figure 10. Intercellular ROS level after treatment with **28** and **41** compared to control cells
***P < 0.001

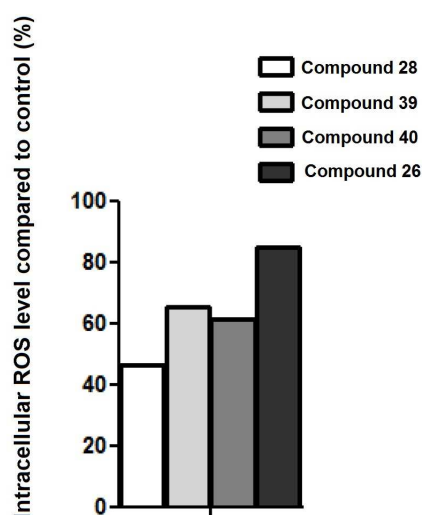


Figure 11. Intracellular ROS level in MCF-7 cells after 24 h treatment with compound **28**, its oxidized analogues **39** and **40**, and compound **26** at 25 μ M compared to control cells.

In addition, we examined effects on apoptosis after 24 h treatment for sulfoxide and sulfonyl analogues of **28**, the compounds **39** and **40**, respectively, at 25 μ M (Figure 12). In spite of the lack of activity shown in vitro in MTT assay (Table 2) derivatives **39** and **40** exhibited significant pro-apoptotic activity against MCF-7 cells. The results indicate that oxidation of sulfur at RS-C(6) did not affect apoptosis-inducing properties of parent compound **28**.

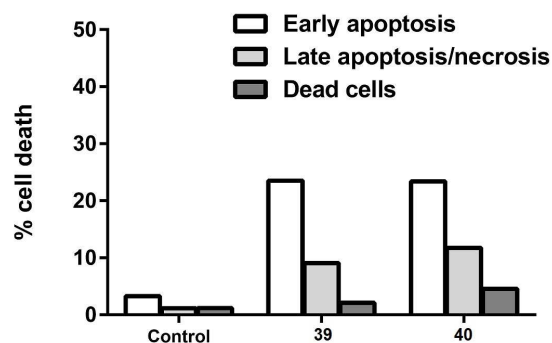


Figure 12. Effects of compounds **39** and **40** on apoptosis in terms of Annexin-V and PI staining of MCF-7 cells upon 24 h treatment

3.1.6. Treatment of NT2/D1 cells with compounds **28** and **30** induced cell detachment and delayed apoptosis

In order to reveal mechanism of extreme sensitivity of NT2/D1 cells to the compounds **28** and **30** we examined their apoptotic effect using bivariate Annexin V-FITC/PI flow cytometry. After 24 h treatment with compounds **28** and **30** at IC₅₀ concentration, NT2/D1 apoptotic response was not observed. Interestingly, we observed massive detachment of NT2/D1 cells seen in cell cultures 24 h after the treatment with both compounds at concentration of 1 μ M (Figure 13).

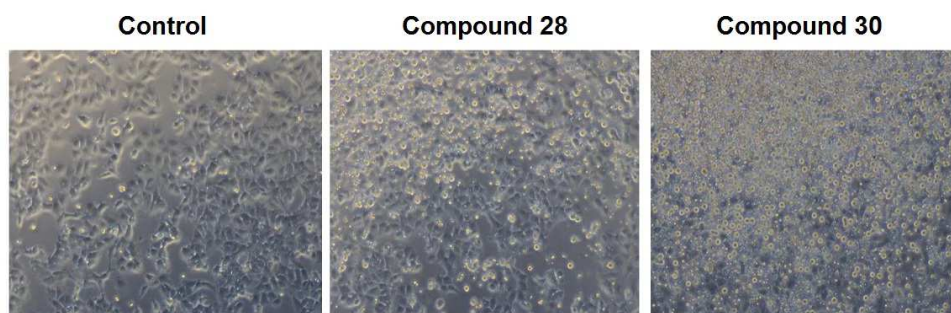


Figure 13. Detachment of NT2/D1 cells upon 24 h of treatment with 1 μ M of compounds **28** and **30**

To further investigate the observed massive cell detachment, progression of apoptosis was analyzed separately in both harvested floating and adherent NT2/D1 cells after 24 h and 48 h treatment with 1 μ M of compounds **28** and **30**. Time-course of apoptotic events was similar for both analyzed compounds (Figure 14). In the sub-population of adherent cells, less than 10% of cells underwent apoptosis in both examined time points (24 h and 48 h treatments). In contrast, floating cells showed higher apoptotic response. At 24 h time point ~20% of cells were in early apoptosis and ~50% in late apoptosis stage. After 48 h treatment,

this ratio was increased in favor of late apoptotic cells (~10% early apoptotic cells and ~80% in late apoptosis) showing that both compounds affect cell adhesion and lead to the rapid induction of the cell death.

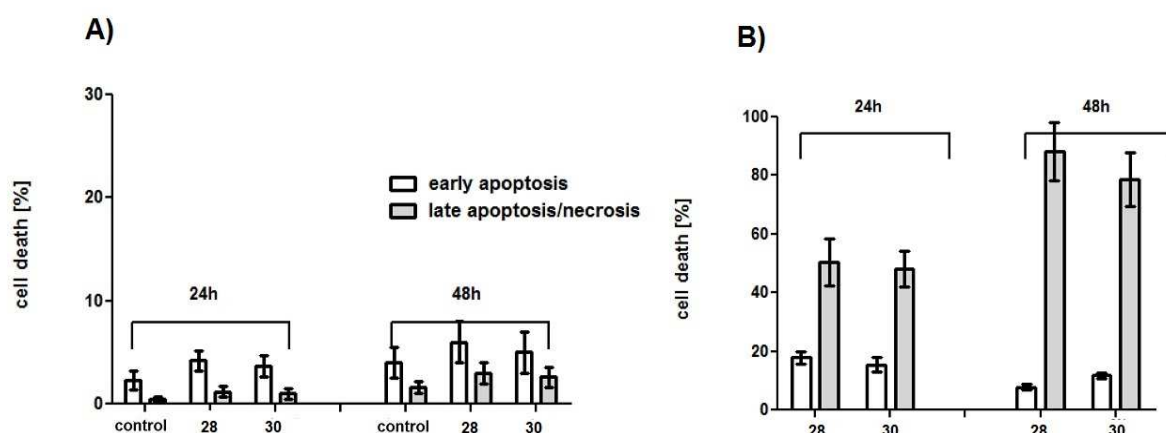


Figure 14. Effects of compounds **28** and **30** on apoptosis of (A) adherent and (B) floating NT2/D1 cells upon 24 h and 48 h of treatment

Detached cells that underwent apoptosis in later stages, point to the anoikis as a mechanism of NT2/D1 cell death. To analyze this outcome in more details we performed trypan blue exclusion test of cell viability³⁶ and count the number of adherent and floating cells (Table 3). Experiments carried out with the concentration of 1 μ M of both, **28** and **30** compounds, revealed that a high number of floating cells (42% and 79%, respectively) was present in the cultures after 24 h of treatment (Table 3); 29% of them were alive after treatment with compound **28** and even more (61%) after treatment with compound **30**. As exposure proceeded, number of floating cell increased to 69% in **28** treated cultures and up to 91% in cells treated with compound **30** but number of live floating cells markedly decreased (15% in **28** treatments and 32% in **30** treatments). **Table 3.** NT2/D1 cell survival and adhesion after treatment with compounds **28** and **30** counted with trypan blue exclusion assay.

Time (h)	28				30				
	Control adherent ^a	Adherent ^a	Floating ^a	Floating % ^b	Live floating % ^c	Adherent ^a	Floating ^a	Floating % ^b	Live floating % ^c
24	52 \pm 9	32 \pm 10	23 \pm 2	42	29	11 \pm 3	42 \pm 7	79	61
48	113 \pm 13	24 \pm 6	54 \pm 4	69	15	4 \pm 2	41 \pm 5	91	32

^a number of cells $\times 10^4$;

^b % floating over total cell number;

^c % live cells over the floating cell number. Data are presented as the mean \pm SD of three independent experiments.

These results suggest that tested carbamates **28** and **30** induced NT2/D1 cell growth inhibition accompanied with detachment from the surface and delayed apoptosis. All these characteristics present hallmarks of anoikis.³⁷ Anoikis triggered by loss of cell anchorage is of

great relevance for many physiological processes while anchorage-independency and resistance to anoikis led to various pathological conditions including metastasis.³⁸

Further examination of antiproliferative effects on NT2/D1 cells showed that 24 h treatment with 1 μ M of compounds **28** and **30** caused accumulation of the cells in G2/M phase (Supplementary material I). Apoptosis induced in NT2/D1 cells involved mitochondrial membrane potential reduction and both tested benzothiazole derivatives, **28** and **30**, significantly decreased ROS level after 48 h treatment (Supplementary material I). These results indicated that carbamate **28** induced very similar pattern of cellular response in both NT2/D1 and MCF-7 cell lines.

3.1.7. Benzothiazole derivatives significantly inhibited formation and growth of NT2/D1 colonies

Next, we checked the effect of examined compounds and the subsequent loss of anchorage on malignant capacity of NT2/D1 cells. We investigated the effect of tested compounds on colony formation and growth, as well as on migration and invasion capacity of NT2/D1 cells.

Colony assays were performed in order to evaluate the effect of carbamates **28** and **30** on NT2/D1 cells colony formation and on colony growth. In colony forming assay cells were seeded and immediately treated with compounds at IC₅₀ concentrations, and colonies formed after seven days were stained and counted. As shown in Figure 15A the treatment with both compounds led to significant reduction in the number of colonies, as compared with control. The inhibitory effect of **30** (~70% inhibition) on colony formation of NT2/D1 cells was higher than that of **28** (~40% inhibition).

In colony growing assay, colonies containing ~10 cells were treated with compounds **28** and **30** and counted when colonies in control untreated NT2/D1 comprised ~50 cells. Decrease of 45% and 25% in the number of large colonies were detected following the treatments with compounds **28** and **30**, respectively (Figure 15 B). These results showed that compounds **28** and **30** have inhibitory potential on the formation and growth of NT2/D1 cell colonies.

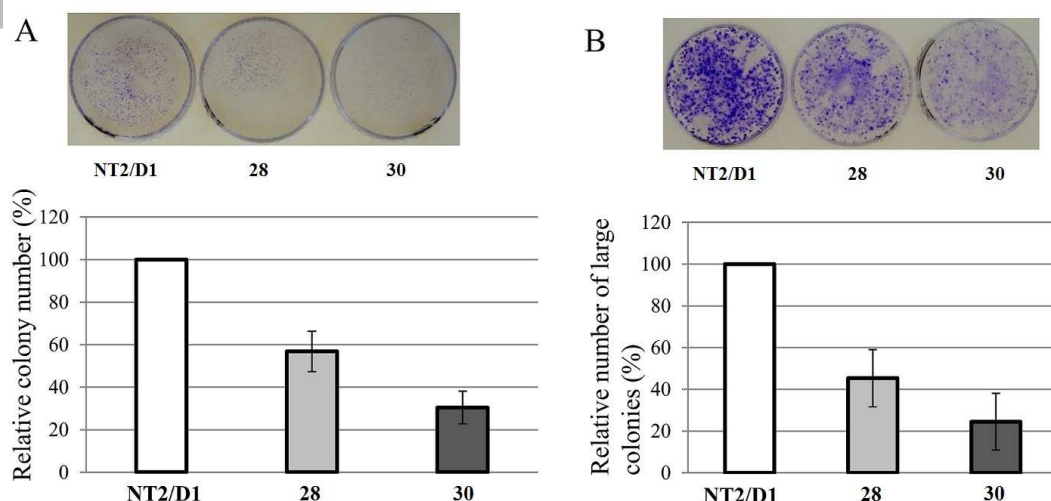


Figure 15. Effects of compounds **28** and **30** on NT2/D1 cells colony formation (A) and colony growth. (B) Representative colonies are shown. The relative number of colonies was calculated as a percentage of the number of colonies of untreated NT2/D1 cells that was set as 100%. Results were presented as the means \pm SEM of two independent experiments

3.1.8. Cell migration

In order to evaluate the impact of compounds **28** and **30** on the migration potential of NT2/D1 cells, we used scratch wound healing assay. NT2/D1 cells were grown to near confluency, wounded and subsequently treated with IC₅₀ concentrations of **28** and **30** or vehicle control (DMSO). Images of wounds were captured immediately after scratches (0 h) and 20 h post-wounding to measure the number of cells invading the denuding zone. As shown in Figure 16, treatments with compounds **28** and **30** decreased migratory potential of NT2/D1 cells to approximately 60% and 40%, respectively compared to control.

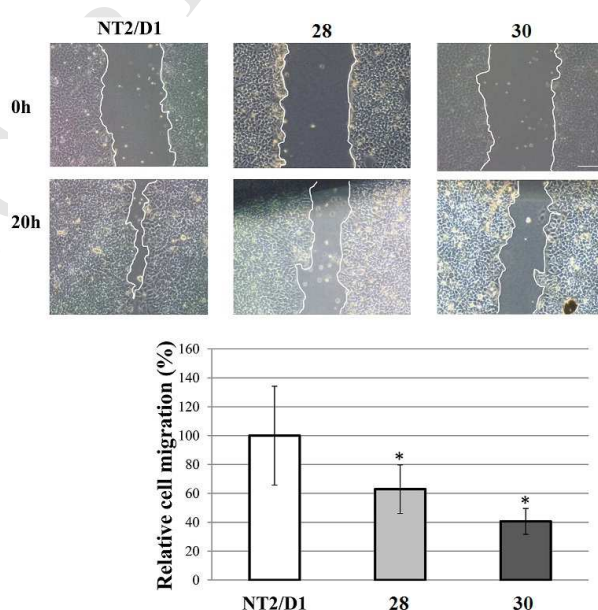


Figure 16. Effects of compounds **28** and **30** on the migratory potential of NT2/D1 cells. The wound healing assay of NT2/D1 cells treated with vehicle control (NT2/D1), compound **28**

and compound **30**. Representative images of the wounds were captured at the indicated time points. The number of treated cells migrated in the denuded area were presented as the percentage of the number of untreated NT2/D1 cells that was set as 100%. The error bars indicate the standard error of the mean. Experiments were performed in triplicate (*P < 0.01). Scale bar: 100 mm

3.1.9. Invasion potential of NT2/D1 cells after treatment with benzothiazole derivatives

To investigate whether cell detachment induced by compounds **28** and **30** is associated with metastatic activity of NT2/D1 cells, we examined the invasive potential of NT2/D1 cells after treatment with tested compounds. NT2/D1 cells were treated with sub-apoptotic IC₅₀ concentrations of **28** and **30** in complete medium for 24 h and seeded to Matrigel coated transwell inserts in serum-free medium. FBS was used as chemoattractant. Cells were allowed to invade for 48 h. As shown in Figure 17, both compounds suppressed NT2/D1 cell invasion reaching 70% inhibition for **28** and even 95% inhibition for compound **30**.

Altogether, results obtained by wound healing assay and cell invasion test demonstrated profound anti-metastatic potential of carbamates **28** and **30** against NT2/D1 cells.

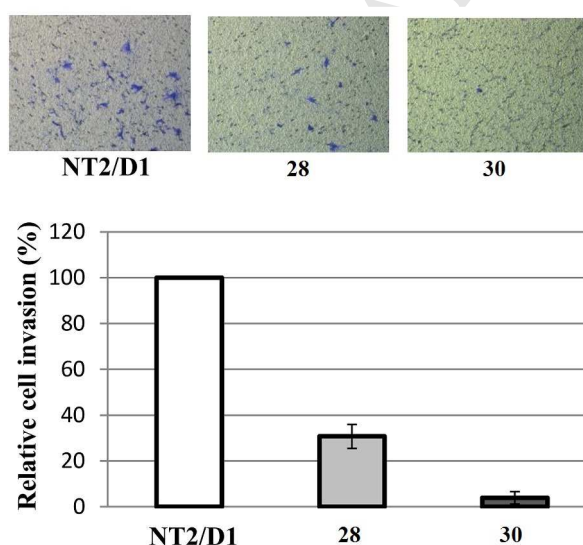


Figure 17. Transwell invasion assay on NT2/D1 cells treated with compounds **28** and **30**. NT2/D1 cells were treated with compounds **28** and **30** in complete culture medium for 24 h and seeded in serum-free medium to transwell inserts (8 mm pore size) coated with Matrigel. After 48 h, untreated and treated invading cells were fixed, stained, and counted microscopically. Representative images of transwell invasion assays were presented. The relative change in cells invasion was calculated as a percentage of the invasion of untreated NT2 cells that was set as 100%. Cells were counted from five fields and averages were calculated. Results were presented as the means \pm SEM of two independent experiments.

3.1.10. In vivo NCI acute toxicity determination

ACCEPTED MANUSCRIPT

After NCI in vitro screening on 60 cell lines panel, compounds **28** and **30** were selected for determination of maximum tolerated dose in a nontumored animal toxicity assay. After i.p. administrated single injection to a female athymic nude mice, examined compounds proved to be nontoxic at the given doses during observation period of 14 days (Supplementary material). Compound **28** showed to be nontoxic at 200 mg/kg dose and compound **30** at 400 mg/kg dose.

4. Discussion

Our newly synthesized benzothiazole derivatives showed antiproliferative activity in vitro against a broad spectrum of human cancer cell lines. Moreover, lack of toxicity of selected compounds in vitro against MRC-5 cell line as well as in vivo, encouraged us to investigate the possible mechanistic pathways underlying observed bioactivity. We selected MCF-7 human breast cell line and NT2/D1 human testicular embryonal carcinoma cells for further experiments. Parallel investigation was performed for carbamate **28** and amide **41** as the most potent compounds against selected MCF-7 cell line and for carbamates **28** and **30** against NT2/D1 cells.

The results obtained on MCF-7 cells demonstrate that compounds **28** and **41** caused the growth inhibition of tumor cells and an apparent block in G2/M cell cycle phase (24 h), subsequently resulting in massive cell accumulation in sub-G1 phase after 48 h treatment. Cell cycle progression is mediated by phosphorylation of different substrates by cyclin dependent kinases (Cdks) at a specific cell cycle phase. Cyclin B1, one of proteins that regulate cell division is mostly cytoplasmic, and it enters nucleus at the end of G2 phase.³⁹ In our study the level of cyclin B1 increased after 24 h and the percentage of cells arrested in G2/M phase was elevated after treatment with two selected compounds, as detected by flow cytometric analysis.

Cell growth inhibition by early apoptosis is one of the preferred modes of anticancer action of therapeutics, mostly because of inducing fewer side effects compared to other types of cell death.⁴⁰ Presented results indicate that examined benzothiazole derivatives were able to induce time-dependent apoptosis in the human breast cancer MCF-7 cells. Moreover, insight into the signaling mechanisms that underlie benzothiazole-induced apoptosis was provided. Mitochondrial dysfunction could be an early event preceding apoptosis.⁴¹ It is characterized by an increase in mitochondrial membrane permeability and loss of membrane potential. Indeed, our data revealed that more than 80% of MCF-7 cells upon 48 h treatment with compounds **28** and **41** exhibited dissipation of mitochondrial membrane potential (Figure 7) and an increase of Bax/Bcl-2 ratio (Figure 8), confirming the completion of the apoptotic program upon G2/M arrest.

molecule plays role in activating the expression and function of numerous pro-apoptotic genes, typically followed by intrinsic cell death pathway.⁴² Persistently increased level of p53 up to 48 h in MCF-7 cells treated with examined benzothiazole derivatives may indicate that apoptosis induced by those compounds is p53 dependent. Unexpectedly, the expression level of p73, another member of p53 family of transcription factors, decreased compared to control cells at both measuring time points. We speculate that significant down-regulation of p73 along with remarkable induction of p53 could be explained assuming that some of caspases cleaved the p73 protein during apoptosis.⁴³ Since MCF-7 cells lack caspase-3,⁴⁴ the cleavage of p73 could be mediated by other executioner caspases, -6 or -7.

Production of reactive oxygen species is increased in cancer cells and those species participate in tumor initiation, progression and maintenance.⁴⁵ Decreasing intracellular ROS levels is known method for inhibiting cancer growth, by modulating many physiological processes that are relevant to cancer growth and ROS are required for those processes.⁴⁶ In addition, suppressing ROS production could prevent the ROS from spreading and protect adjacent healthy cells from oxidative DNA damage, consequently diminishing toxic side effects of cancer therapy.⁴⁷ We found that tested compounds significantly decrease the production of ROS in MCF-7 cells after treatment. A comparative study of **28** and analogues **39** and **40** indicated that RS-C(6) substituent is important for suppressing ROS accumulation in MCF-7 cells, in addition to thiazole sulfur due to their overall antioxidative contribution.

Considering the obtained results, it is worth to notice that, in spite of functional group difference between the two test compounds used in this study, carbamate **28** and amide **41**, our findings indicated that both follow the same mechanism of action against MCF-7 cancer cell line.

The results obtained on NT2/D1 cell line indicated that carbamates **28** and **30** induced cell growth inhibition and triggered cell detachment from the substrate accompanied with apoptosis. These sequence of events is characteristic of a particular type of apoptosis, designated as anoikis.^{48,49} The occurrence of anoikis is supported by the high number of floating live cells followed by detected apoptosis.^{37,49}

Cell detachment is probably caused by the aberrant regulation of cell adhesion and further investigation is needed to elucidate exact mechanism of carbamates' action used in this study. Although some differences in the degree of cellular response to compounds **28** and **30** have been detected, it is likely that both compounds engaged the same molecular mechanisms in NT2/D1 cells. Different cellular responses of MCF-7 and NT2/D1 to carbamate **28** probably reflects diverse interactions of **28** in different cellular context. It suggests that cell detachment and delayed apoptosis may be limited to testicular cancer cells

and does not represent common mechanism in other cancer cells. Nevertheless, tested compounds induced very similar response in terms of cell cycle arrest, mitochondrial involvement in apoptosis and ROS affection in both MCF-7 and NT2/D1 cell lines.

Anoikis is potential target for new anticancer therapies approaches as a signal for cancer cell death induced by cell detachment.⁵⁰ The only consideration about these approaches is potential metastatic spread following cell detachment.³⁷ Induction of NT2/D1 cell detachment and observed restriction in cell viability and growth, together with a reduction in cell invasiveness and ability to migrate, marked compounds **28** and **30** as promising new compounds that need further validation as potential effective therapeutic agents. Since NT2/D1 cells showed exceptional sensitivity to the tested carbamates and that compounds **28** and **30** had no cytotoxic effect on control cells and in non-tumored mice, it would be interesting to analyze the potential synergistic effect of these compounds and cisplatin in future study. Cisplatin-based chemotherapy is the most efficient treatment of testicular germ cell tumors⁵¹ but its clinical application may be limited due to its toxicity and resistance.⁵² To minimize these effects, there is constant search for new combinatorial therapies that could reduce common side effects of platinum based chemotherapeutic drugs and its effective dose.⁵³ Further studies would evaluate the potential use of compound **28** and/or **30** in combinatorial treatment of testicular carcinoma.

In a last few years testicular carcinoma NT2/D1 cells are being considered as cancer stem cells (CSC), a subpopulation of cancer cells responsible for tumor growth, progression and its metastatic spreading.^{54,55} CSCs are considered responsible for tumor resistance to chemo- and radiotherapies and consequent failure of conventional therapeutic approaches.⁵⁴ Therefore, targeting unique features of CSCs is another ultimate goal of cancer treatment research. These approaches include pluripotency restriction, induction of differentiation and sensitization to particular compound.⁵⁶ To elucidate whether tested carbamates **28** and **30** may be candidates for these strategies further investigations are needed.

5. Conclusion

Synthesized benzothiazole derivatives showed good potency against proliferation of various cancer cell lines in vitro. In this study it was demonstrated that synthesized propyl [6-(propylsulfanyl)-1,3-benzothiazol-2-yl]carbamate **28** and *N*-[6-(propylsulfanyl)-1,3-benzothiazol-2-yl]pentanamide **41**, selected for mechanistic evaluation of activity against MCF-7, exhibit their antiproliferative activity by blocking cell cycle in G2/M phase and by promoting apoptosis. Apoptotic cell death was further determined with mitochondrial membrane potential reduction and increased Bax/Bcl-2 ratio after treatment of MCF-7 cells with selected benzothiazoles, along with induction of p53. While the most of strategies for

cancer therapies based on affecting ROS and apoptosis consider induction of ROS production,⁵⁷ compounds tested in this study showed significant reduction of ROS accumulation. In addition, two most potent derivatives, carbamate **28** and propyl [6-(butylsulfanyl)-1,3-benzothiazol-2-yl]carbamate **30** exhibited significant antiproliferative activity against NT2/D1 cell line. The massive detachment of the NT2/D1 cells after treatment with compounds **28** and **30** accompanied with apoptosis and inhibitory activity against migration and invasiveness of these cells were shown. Moreover, derivatives **28**, **30** and **41** were nontoxic against normal MRC-5 cells in vitro, and the most potent compounds **28** and **30** showed no toxicity in non-tumored animal toxicity assay. Further studies are needed to clarify the precise targets for antiproliferative and antimigratory activity of aminobenzothiazole derivatives on NT2/D1 cells, as well as new aspects for possible improvement of current therapies.

6. Experimental section

6.1. General information

Melting points were determined on a Boetius PMHK apparatus and were not corrected. IR spectra were taken on a Thermo-Scientific Nicolet 6700 FT-IR diamond crystal. NMR: ¹H and ¹³C NMR spectra were recorded on a Bruker Ultrashield Advance III spectrometer (at 500 and 125 MHz, respectively) in the indicated solvent using TMS as the internal standard. Chemical shifts are expressed in ppm (δ) values, and coupling constants (J), in Hz. ESI MS spectra of the synthesized compounds were recorded on an Agilent Technologies 6210 time-of-flight LC/MS instrument in positive ion mode using CH₃CN/H₂O = 1/1 with 0.2% HCOOH as the carrying solvent solution. The samples were dissolved in pure methanol (HPLC grade). The selected values were as follows: capillary voltage = 4 kV; gas temperature 350 °C; drying gas = 12 L min⁻¹; nebulizer pressure = 45 psig; and fragmentator voltage = 70 V. The flash chromatography was performed on Biotage SP1 system equipped with UV detector and FLASH 12+, FLASH 25+ or FLASH 40+ columns charged with KP-SIL (40 – 63 μ m, pore diameter 60 Å), KP-C18-HS (40 – 63 μ m, pore diameter 90 Å) or KP-NH (40 – 63 μ m, pore diameter 100 Å) as an adsorbent. Compounds were analyzed for purity (HPLC) using Agilent 1200 HPLC system equipped with a Quat Pump (G1311B), an injector (G1329B) 1260 ALS, TCC 1260 (G1316A) and a detector 1260 DAD VL+ (G1315C). All tested compounds are fully characterized and the purities were > 95% as determined by HPLC (Supplementary material). HPLC analysis was performed in two diverse systems for each compound. Compounds were dissolved in methanol, final concentrations were ~ 1mg/mL. Applied HPLC methods were as follows.

Method A. Zorbax Eclipse Plus C18 4.6 × 150mm, 1.8μ, S.N. USWKY01594 was used as the stationary phase. Eluent was made of the following solvents: 0.2% formic acid in water (A) and acetonitrile (B). The analysis were performed at 280 nm for compounds **23 – 26** and **29 – 31**; at 290 nm for compounds **28, 33, 34** and **41** and at 320 nm for compounds **42 – 46**. Flow rate was 0.5 mL/min.

Method B. Zorbax Eclipse Plus C18 4.6 × 150mm, 1.8μ, S.N. USWKY01594 was used as the stationary phase. Eluent was made of the following solvents: 0.2% formic acid in water (A) and methanol (B). The analysis were performed at 280 nm for compounds **24 – 26** and **29 – 31**; at 290 nm for compounds **28, 34** and **41** and at 320 nm for compounds **32** and **42 – 46**. Flow rate was 0.5 mL/min.

Method C. Zorbax Eclipse Plus C18 2.1 × 100mm, 1.8μ, S.N. USUXU04444 was used as the stationary phase. Eluent was made of the following solvents: water (A) and methanol (B). The analysis were performed at 320 nm for compound **32**. Flow rate was 0.5 mL/min.

Method D. Poroshell 120 EC-C18, 4.6 × 50mm, 2.7μ, S.N. USCFU07797 was used as the stationary phase. Eluent was made of the following solvents: 0.2% formic acid in water (A) and acetonitrile (B). The analysis were performed at 290 nm for compound **33** and 280 nm for compounds **27** and **38**. Flow rate was 1 mL/min.

Method E. Zorbax Eclipse Plus C18 4.6 × 150mm, 1.8μ, S.N. USWKY01594 was used as the stationary phase. Eluent was made of the following solvents: water (A) and acetonitrile (B). The analysis were performed at 280 nm for compound **37** and at 290 nm for compounds **35** and **36**. Flow rate was 0.5 mL/min.

Method F. Zorbax Eclipse Plus C18 4.6 × 150mm, 1.8μ, S.N. USWKY01594 was used as the stationary phase. Eluent was made of the following solvents: water (A) and methanol (B). The analysis were performed at 290 nm for compounds **35** and **36** and at 280 nm for compound **37**. Flow rate was 0.5 mL/min.

Method G. Zorbax Eclipse Plus C18 2.1 × 100mm, 1.8μ, S.N. USUXU04444 was used as the stationary phase. Eluent was made of the following solvents: 0.2% formic acid in water (A) and methanol (B). The analysis were performed at 295 nm for compounds **39** and **40**. Flow rate was 0.5 mL/min.

Method H. Zorbax Eclipse Plus C18 2.1 × 100mm, 1.8μ, S.N. USUXU04444 was used as the stationary phase. Eluent was made of the following solvents: 0.2% formic acid in water (A) and acetonitrile (B). The analysis were performed at 295 nm for compound **39**. Flow rate was 0.5 mL/min.

Method I. Poroshell 120 EC-C18, 4.6 × 50mm, 2.7μ, S.N. USCFU07797 was used as the stationary phase. Eluent was made of the following solvents: 0.2% formic acid in water (A)

and methanol (B). The analysis were performed at 280 nm for compounds **27** and **38** and 295 nm for compound **40**. Flow rate was 0.5 mL/min.

6.2. Chemical synthesis

6.2.1. General procedure C for synthesis of (6-Substituted-1,3-benzo[d]thiazol-2-yl)carbamates **24** – **26**, **29**, **31** and **32**

A solution of bromine (1.25 eq) in glacial acetic acid was added to a stirring mixture of an appropriate 4-substituted aniline (1 eq), ammonium thiocyanate (4 eq), acetic acid and water at 10 °C. The reaction mixture was stirred at room temperature for 18 h, and then at 80 °C for 3 h. After cooling to room temperature, the reaction mixture was poured onto water and Na₂CO₃ was added in order to adjust pH to 5-6. The reaction mixture was extracted with ethyl acetate, layers were separated and organic layer was washed with brine. Organic layer was dried over anhydrous Na₂SO₄, filtered and evaporated to dryness. The crude product 6-substituted aminobenzothiazole was used in the next reaction step. An appropriate alkyl chloroformate (1.1 eq) and triethylamine (1.8 eq) were added to a solution of 6-substituted aminobenzothiazole in benzene. The reaction mixture was stirred at 80°C for 3 h, and then poured onto cold water and extracted with ethyl acetate. Combined organic layers were dried over anhydrous Na₂SO₄, filtered and evaporated to dryness. The crude product was further purified in a manner provided for each compound.

6.2.1.1. Ethyl [6-(ethylsulfanyl)-1,3-benzothiazol-2-yl]carbamate (24). Yield 40%. M.p. = (162 – 165) °C. IR (ATR): 3432w, 3400w, 3162m, 3124m, 3079m, 3045m, 2973s, 2924s, 2776m, 1720s, 1599s, 1557s, 1444s, 1364m, 1290s, 1250s, 1119m, 1070m, 1048m, 1021w, 820m, 757m cm⁻¹. ¹H NMR (500 MHz, (CD₃)₂SO, δ): 7.96 (d, *J* = 1.6 Hz, 1H), 7.61 (d, *J* = 8.4 Hz, 1H), 7.36 (dd, *J*₁ = 8.4 Hz, *J*₂ = 1.8 Hz, 1H), 4.24 (q, *J* = 7.1 Hz, 2H), 2.98 (q, *J* = 7.3 Hz, 2H), 1.28 (t, *J* = 7.1 Hz, 3H), 1.22 (t, *J* = 7.3 Hz, 3H). ¹³C NMR (125 MHz, (CD₃)₂SO, δ): 159.53, 153.88, 147.84; 132.61, 130.26, 127.58, 121.85, 120.52, 61.94, 27.48, 14.30. (+)ESI-HRMS: *m/z* 283.05655 corresponds to molecular formula C₁₂H₁₄N₂O₂S₂H⁺ (error, -1.38 ppm). HPLC purity, method A: *t*_R = 8.695, area 99.27%. Method B: *t*_R = 9.906, area 96.29%.

6.2.1.2. Ethyl [6-(propylsulfanyl)-1,3-benzothiazol-2-yl]carbamate (25). Yield 21%. M.p. = (158 – 162) °C. IR (ATR): 3135w, 3076w, 2957m, 2909m, 2869m, 2782m, 1725s, 1597s, 1561s, 1453s, 1428m, 1270s, 1243s, 1110m, 1069m, 1045m, 1022m, 816m, 759m, 707m cm⁻¹. ¹H NMR (500 MHz, (CD₃)₂SO, δ): 12.00 (bs, 1H), 7.96 (d, *J* = 1.4 Hz, 1H), 7.60 (d, *J* = 8.5 Hz, 1 H), 7.36 (dd, *J*₁ = 8.5 Hz, *J*₂ = 1.8 Hz, 1H), 4.24 (q, *J* = 7.1 Hz, 2H), 2.94 (t, *J* = 7.1 Hz, 2H), 1.61 – 1.54 (m, 2H), 1.27 (t, *J* = 7.1 Hz, 3H), 0.96 (t, *J* = 7.3 Hz, 3H). ¹³C NMR (50 MHz, (CD₃)₂SO, δ): 159.85, 154.23, 148.00, 132.89, 130.76, 127.84, 122.09, 120.78, 62.20, 35.57, 22.22, 14.52, 13.34. (+)ESI-HRMS: *m/z* 297.07191 corresponds to molecular formula

$C_{13}H_{16}N_2O_2S_2H^+$ (error, -2.30 ppm). HPLC purity, method A: $t_R = 9.194$, area 99.67%.

Method B: $t_R = 10.528$, area 99.44%.

6.2.1.3. Propyl (6-ethoxy-1,3-benzothiazol-2-yl)carbamate (26). Yield 25%. M.p. = (168 – 169) °C. IR (ATR): 3161w, 3081m, 2977s, 2933m, 2802m, 1718s, 1612s, 1562s, 1463s, 1391m, 1272s, 1242s, 1212s, 1113m, 1057s, 971w, 941m, 792m, 760m cm^{-1} . 1H NMR (500 MHz, $(CD_3)_2SO$, δ): 11.83 (bs, 1H), 7.56 (d, $J = 8.9$ Hz, 1H), 7.51 (d, $J = 2.5$ Hz, 1H), 6.97 (dd, $J_1 = 8.7$ Hz, $J_2 = 2.5$ Hz, 1H), 4.14 (t, $J = 6.6$ Hz, 1H), 4.04 (q, $J = 7.0$ Hz, 2H), 1.69 – 1.62 (m, 2H), 1.33 (t, $J = 6.9$ Hz, 3H), 0.93 (t, $J = 7.5$ Hz, 3H). ^{13}C NMR (125 MHz, $(CD_3)_2SO$, δ): 157.46, 155.12, 143.28, 132.76, 120.81, 114.97, 105.47, 67.16, 63.62, 21.73, 14.70, 10.13. (+)ESI-HRMS: m/z 281.09541 corresponds to molecular formula $C_{13}H_{16}N_2O_3SH^+$ (error, -0.10 ppm). HPLC purity, method A: $t_R = 8.520$, area 99.48%. Method B: $t_R = 9.741$, area 96.69%.

6.2.1.4. Ethyl [6-(butylsulfanyl)-1,3-benzothiazol-2-yl]carbamate (29). Yield 19%. M.p. = (138 – 140) °C. IR (ATR): 3139m, 3072s, 2983s, 2954s, 2931s, 2865s, 2794s, 1724s, 1603s, 1570s, 1452s, 1366m, 1340m, 1313m, 1293s, 1274s, 1250s, 1113m, 1070m, 1048m, 1022m, 816s, 781m, 760s, 708m cm^{-1} . 1H NMR (500 MHz, $CDCl_3$, δ): 11.90 (bs, 1H), 7.86 (d, $J = 8.6$ Hz, 1H), 7.78 (d, $J = 1.7$ Hz, 1H), 7.40 (dd, $J_1 = 8.4$ Hz, $J_2 = 1.8$ Hz, 1H), 4.41 (q, $J = 7.3$ Hz, 2H), 2.96 (t, $J = 7.5$ Hz, 2H), 1.67 – 1.61 (m, 2H), 1.50 – 1.41 (m, 5H), 0.93 (t, $J = 7.3$ Hz, 3H). ^{13}C NMR (125 MHz, $(CD_3)_2SO$, δ): 161.39, 153.81, 147.21, 132.40, 131.82, 128.33, 122.21, 120.81, 62.88, 34.73, 31.28, 21.89, 14.46, 13.63. (+)ESI-HRMS: m/z 311.08801 corresponds to molecular formula $C_{14}H_{18}N_2O_2S_2H^+$ (error, -0.76 ppm). HPLC purity, method A: $t_R = 9.757$, area 97.08%. Method B: $t_R = 11.594$, area 96.14%.

6.2.1.5. Butyl [6-(propylsulfanyl)-1,3-benzothiazol-2-yl]carbamate (31). Yield 28%. M.p. = (74 – 80) °C. IR (ATR): 3170m, 3070m, 2961s, 2931s, 2872m, 1721s, 1602s, 1562s, 1456m, 1293s, 1248s, 1074w, 814w, 762w cm^{-1} . 1H NMR (500 MHz, $(CD_3)_2SO$, δ): 7.94 (d, $J = 1.6$ Hz, 1H), 7.60 (d, $J = 8.3$ Hz, 1H), 7.35 (dd, $J_1 = 8.5$ Hz, $J_2 = 1.8$ Hz, 1H), 4.19 (t, $J = 6.6$ Hz, 2H), 2.94 (t, $J = 7.1$ Hz, 2H), 1.65 – 1.53 (m, 4H), 1.41 – 1.35 (m, 2H), 0.95 (t, $J = 7.3$ Hz, 3H), 0.91 (t, $J = 7.5$ Hz, 3H). ^{13}C NMR (125 MHz, $(CD_3)_2SO$, δ): 159.60, 154.04, 147.74, 132.63, 130.53, 127.60, 121.84, 120.51, 65.59, 35.43, 30.34, 22.02, 18.50, 13.55, 13.11. (+)ESI-HRMS: m/z 325.10391 corresponds to molecular formula $C_{15}H_{20}N_2O_2S_2H^+$ (error, +0.05 ppm). HPLC purity, method A: $t_R = 10.346$, area 99.78%. Method B: $t_R = 11.916$, area 99.36%.

6.2.1.6. Propyl [6-(ethylsulfanyl)-1,3-benzothiazol-2-yl]carbamate (32). Yield 27%. M.p. = (137-138) °C. IR (ATR): 3062m, 2968s, 2922s, 1717s, 1600m, 1562m, 1445m, 1396w, 1287m, 1248m, 1072w, 1044w, 759w cm^{-1} . 1H NMR (500 MHz, $(CD_3)_2SO$, δ): 12.01 (bs, 1H), 7.95 (d, $J = 1.8$ Hz, 1H), 7.61 (d, $J = 8.5$ Hz, 1H), 7.36 (dd, $J_1 = 8.5$ Hz, $J_2 = 1.8$ Hz,

1H), 4.15 (t, $J = 6.8$ Hz, 1H), 2.98 (q, $J = 7.3$ Hz, 2H), 1.70 – 1.63 (m, 2H), 1.22 (t, $J = 7.3$ Hz, 3H), 0.93 (t, $J = 7.5$ Hz, 3H). ^{13}C NMR (125 MHz, $(\text{CD}_3)_2\text{SO}$, δ): 160.13, 154.54, 148.24, 133.06, 130.67, 128.02, 122.27, 120.93, 67.73, 27.93, 22.12, 14.74, 10.56. (+)ESI-HRMS: m/z 297.07243 corresponds to molecular formula $\text{C}_{13}\text{H}_{16}\text{N}_2\text{O}_2\text{S}_2\text{H}^+$ (error, -0.57 ppm). HPLC purity, method B: $t_{\text{R}} = 12.996$, area 95.61%. Method C: $t_{\text{R}} = 14.178$, area 95.09%.

6.2.2. General procedure D for synthesis of compounds 28, 30 and 33 – 37

An appropriate alkyl chloroformate (1.1 eq) and triethylamine (1.8 eq) were added to a solution of corresponding 6-(alkylsulfanyl)-1,3-benzothiazol-2-amine (1 eq) in benzene. After 3 h of stirring at 80 °C the reaction mixture was poured onto water and extracted with ethyl acetate. Combined organic layers were dried over anhydrous Na_2SO_4 , filtered and evaporated to dryness. The crude product was subjected to silica gel column chromatography and silica gel flash chromatography, Biotage SP1, using hexane/ethyl acetate as eluent to afford the final product.

6.2.2.1. Propyl [6-(propylsulfanyl)-1,3-benzothiazol-2-yl]carbamate (28). Yield 47%. M.p. = (138 – 140) °C. IR (ATR): 3167m, 3062m, 2960s, 2932m, 2876m, 1724s, 1598s, 1562s, 1449m, 1447s, 1308m, 1273s, 1244s, 1047m, 962w, 888w, 805m, 782m, 755m cm^{-1} . ^1H NMR (500 MHz, $(\text{CD}_3)_2\text{SO}$, δ): 12.01 (bs, 1H), 7.96 (d, $J = 1.7$ Hz, 1H), 7.60 (d, $J = 8.4$ Hz, 1H), 7.36 (dd, $J_1 = 8.4$ Hz, $J_2 = 1.9$ Hz, 1H), 4.15 (t, $J = 6.7$ Hz, 2H), 2.94 (t, $J = 7.2$ Hz, 2H), 1.70 – 1.63 (m, 2H), 1.61-1.54 (m, 2H), 0.98-0.92 (m, 6H). ^{13}C NMR (125 MHz, $(\text{CD}_3)_2\text{SO}$, δ): 159.54, 154.00, 147.74, 132.61, 130.49, 127.58, 121.82, 120.49, 67.28, 35.38, 21.99, 21.68, 13.09, 10.10. (+)ESI-HRMS: m/z 311.08810 corresponds to molecular formula $\text{C}_{14}\text{H}_{18}\text{N}_2\text{O}_2\text{S}_2\text{H}^+$ (error, -0.47 ppm). HPLC purity, method A: $t_{\text{R}} = 11.532$, area 98.23%. Method B: $t_{\text{R}} = 13.159$, area 98.53%.

6.2.2.2. Propyl [6-(butylsulfanyl)-1,3-benzothiazol-2-yl]carbamate (30). Yield 29%. M.p. = 130 °C. IR (ATR): 3169m, 3068m, 2960s, 2926s, 2785m, 1725s, 1601m, 1564m, 1451m, 1288m, 1247m, 1070w, 818w, 752w cm^{-1} . ^1H NMR (500 MHz, CDCl_3 , δ): 11.35 (bs, 1H), 7.82 (d, $J = 8.5$ Hz, 1H), 7.78 (d, $J = 1.4$ Hz, 1H), 7.40 (dd, $J_1 = 8.5$ Hz, $J_2 = 1.8$ Hz, 1H), 4.30 (t, $J = 6.8$ Hz, 2H), 2.96 (t, $J = 7.4$ Hz, 2H), 1.84 – 1.77 (m, 2H), 1.67 – 1.61 (m, 2H), 1.50 – 1.42 (m, 2H), 0.99 (t, $J = 7.5$ Hz, 3H), 0.92 (t, $J = 7.3$ Hz, 3H). ^{13}C NMR (125 MHz, CDCl_3 , δ): 161.06, 153.80, 147.35, 132.54, 131.83, 128.42, 122.29, 120.83, 68.53, 34.77, 31.31, 22.14, 21.91, 13.65, 10.32. (+)ESI-HRMS: m/z 325.10408 corresponds to molecular formula $\text{C}_{15}\text{H}_{20}\text{N}_2\text{O}_2\text{S}_2\text{H}^+$ (error, +0.56 ppm). HPLC purity, method A: $t_{\text{R}} = 10.371$, area 96.76%. Method B: $t_{\text{R}} = 12.388$, area 98.58%.

6.2.2.3. Ethyl [6-(pentylsulfanyl)-1,3-benzothiazol-2-yl]carbamate (33). Yield 21%. M.p. = (137 – 138) °C. IR (ATR): 3175m, 3152m, 3123m, 3058m, 2956s, 2924s, 2854s, 1724s, 1597s, 1550s, 1460s, 1370m, 1296s, 1241s, 1069m, 818m, 766m cm^{-1} . ^1H NMR (500 MHz,

CDCl₃, δ): 11.60 (bs, 1H), 7.84 (d, $J = 8.5$ Hz, 1H), 7.78 (d, $J = 1.6$ Hz, 1H), 7.40 (dd, $J_1 = 8.5$ Hz, $J_2 = 1.6$ Hz, 1H), 4.40 (q, $J = 7.1$ Hz, 2H), 2.95 (t, $J = 7.5$ Hz, 2H), 1.69 – 1.63 (m, 2H), 1.45 – 1.39 (m, 5H), 1.37 – 1.29 (m, 2H), 0.89 (t, $J = 7.2$ Hz, 3H). ¹³C NMR (125 MHz, CDCl₃, δ): 161.19, 153.75, 147.25, 132.47, 131.85, 128.37, 122.22, 120.82, 62.90, 35.01, 30.93, 28.88, 22.23, 14.46, 13.94. (+)ESI-HRMS: m/z 325.10435 corresponds to molecular formula C₁₅H₂₀N₂O₂S₂H⁺ (error, +1.40 ppm). HPLC purity, method A: $t_R = 12.206$, area 98.52%. Method D: $t_R = 4.563$, area 98.28%.

6.2.2.4. Propyl [6-(pentylsulfanyl)-1,3-benzothiazol-2-yl]carbamate (34). Yield 40%. M.p. = (116 – 118) °C. IR (ATR): 3170m, 3127m, 3062m, 2956s, 2923s, 2853s, 2784m, 1725s, 1601s, 1562s, 1451m, 1393m, 1309m, 1289s, 1248s, 1069m, 821m, 752m cm⁻¹. ¹H NMR (500 MHz, CDCl₃, δ): 11.72 (bs, 1H), 7.84 (d, $J = 8.6$ Hz, 1H), 7.78 (d, $J = 1.5$ Hz, 1H), 7.40 (dd, $J_1 = 8.4$ Hz, $J_2 = 1.8$ Hz, 1H), 4.30 (t, $J = 6.8$ Hz, 2H), 2.94 (t, $J = 7.4$ Hz, 2H), 1.84 – 1.77 (m, 2H), 1.69 – 1.63 (m, 2H), 1.45 – 1.39 (m, 2H), 1.36 – 1.29 (m, 2H), 0.99 (t, $J = 7.5$ Hz, 3H), 0.89 (t, $J = 7.2$ Hz, 3H). ¹³C NMR (125 MHz, CDCl₃, δ): 161.31, 153.88, 147.26, 132.43, 131.80, 128.37, 122.23, 120.77, 68.50, 35.03, 30.92, 28.87, 22.22, 22.11, 13.93, 10.30. (+)ESI-HRMS: m/z 339.12006 corresponds to molecular formula C₁₆H₂₂N₂O₂S₂H⁺ (error, +1.51 ppm). HPLC purity, method A: $t_R = 13.079$, area 96.82%. Method B: $t_R = 14.812$, area 95.51%.

6.2.2.5. Ethyl {6-[(2-methylpropyl)sulfanyl]-1,3-benzothiazol-2-yl}carbamate (35). Yield 23%. M.p. = (159 – 160) °C. IR (ATR): 3139m, 3081m, 2968s, 2914s, 2866m, 1722s, 1599s, 1560s, 1458m, 1275s, 1246s, 1111m, 1070m, 1049m, 1019m, 820m, 789m, 762m cm⁻¹. ¹H NMR (500 MHz, CDCl₃, δ): 11.47 (bs, 1H), 7.84 (d, $J = 8.5$ Hz, 1H), 7.77 (d, $J = 1.6$ Hz, 1H), 7.40 (dd, $J_1 = 8.5$ Hz, $J_2 = 1.8$ Hz, 1H), 4.41 (q, $J = 7.1$ Hz, 2H), 2.85 (d, $J = 6.9$ Hz, 2H), 1.88 (sep, $J = 6.7$ Hz, 1H), 1.42 (t, $J = 7.1$ Hz, 3H), 1.05 (d, $J = 6.6$ Hz, 6H). ¹³C NMR (125 MHz, CDCl₃, δ): 161.25, 153.77, 147.18, 132.44, 132.27, 128.30, 122.13, 62.88, 44.10, 28.32, 22.01, 14.46. (+)ESI-HRMS: m/z 311.08796 corresponds to molecular formula C₁₄H₁₈N₂O₂S₂H⁺ (error, -0.92 ppm). HPLC purity, method E: $t_R = 12.189$, area 99.00%. Method B: $t_R = 13.873$, area 99.59%.

6.2.2.6. Propyl {6-[(2-methylpropyl)sulfanyl]-1,3-benzothiazol-2-yl}carbamate (36). Yield 62%. M.p. = (139 – 141) °C. IR (ATR): 3172m, 3131m, 3074m, 2919s, 2852m, 1722s, 1599m, 1565m, 1456m, 1282s, 1245s, 1074m, 818m, 760m cm⁻¹. ¹H NMR (500 MHz, CDCl₃, δ): 11.60 – 11.58 (m, 1H), 7.83 (d, $J = 8.4$ Hz, 1H), 7.77 (d, $J = 1.6$ Hz, 1H), 7.40 (dd, $J_1 = 8.4$ Hz, $J_2 = 1.8$ Hz, 1H), 4.30 (t, $J = 6.8$ Hz, 2H), 2.85 (d, $J = 6.8$ Hz, 2H), 1.91 – 1.77 (m, 3H), 1.05 (d, $J = 6.6$ Hz, 6H), 0.99 (t, $J = 7.43$ Hz, 3H). ¹³C NMR (125 MHz, CDCl₃, δ): 161.18, 153.85, 147.23, 132.47, 132.25, 128.33, 122.16, 120.79, 68.49, 44.11, 28.31, 22.00, 10.30. (+)ESI-HRMS: m/z 325.10387 corresponds to formula C₁₅H₂₀N₂O₂S₂H⁺ (error, -0.08

ppm). HPLC purity, method E: $t_R = 12.787$, area 98.08%. Method F: $t_R = 14.618$, area 99.74%.

6.2.2.7. Butyl [6-(butylsulfanyl)-1,3-benzothiazol-2-yl]carbamate (37). Yield 32%. M.p. = (120-121) °C. IR (ATR): 3143m, 3077m, 2953s, 2928s, 2866m, 1727s, 1598s, 1452m, 1276m, 1246m, 1108w, 1074w, 820m, 782w, 756m, cm^{-1} . ^1H NMR (500 MHz, CDCl_3 , δ): 11.64 – 11.41 (m, 1H), 7.84 – 7.81 (m, 1H), 7.78 (d, $J = 1.5$ Hz, 1H), 7.40 (dd, $J_1 = 8.6$ Hz, $J_2 = 1.7$ Hz, 1H), 4.35 (t, $J = 6.7$ Hz, 2H), 2.96 (t, $J = 7.4$ Hz, 2H), 1.79 – 1.73 (m, 2H), 1.67 – 1.61 (m, 2H), 1.50 – 1.38 (m, 4H), 0.97 – 0.91 (m, 6H). ^{13}C NMR (125 MHz, CDCl_3 , δ): 161.50, 153.95, 147.22, 132.39, 131.77, 128.33, 122.25, 120.76, 66.76, 34.75, 31.28, 30.76, 21.88, 18.99, 13.66. (+)ESI-HRMS: m/z 339.12048 corresponds to molecular formula $\text{C}_{16}\text{H}_{22}\text{N}_2\text{O}_2\text{S}_2\text{H}^+$ (error, +2.77 ppm). HPLC purity, method E: $t_R = 12.749$, area 95.92%. Method F: $t_R = 14.577$, area 98.25%.

6.2.3. General procedure E for synthesis of *N*-[6-(Propylsulfanyl)-1,3-benzothiazol-2-yl]alkanamides 41 – 46

The alkanoyl chlorides were prepared according to known procedures using an appropriate commercially available acids and thionyl chloride as starting materials.⁵⁸ A solution of an appropriate alkanoyl chloride (1.3 eq) in benzene was added dropwise into the solution of corresponding aminobenzothiazole (1 eq) (**19** or **20**) in CH_2Cl_2 /benzene (1:1, v/v) at 0 °C. The reaction mixture was stirred at the same temperature until consumption of starting aminobenzothiazole (TLC control). The reaction was quenched with cold water. The layers were separated and the aqueous layer was extracted with CH_2Cl_2 . The combined organic layers were dried over anhydrous Na_2SO_4 , filtered and evaporated to dryness. The crude product was subjected to a multiple column chromatography to afford desired compound.

6.2.3.1. *N*-[6-(propylsulfanyl)-1,3-benzothiazol-2-yl]pentanamide (41). Yield 21%. M.p. = 113 °C. IR (ATR): 3276m, 3178m, 3128m, 3064m, 2960s, 2930m, 2870m, 1660s, 1594s, 1538s, 1439m, 1374w, 1345m, 1295m, 1266m, 1192w, 1087w, 815w, 774w cm^{-1} . ^1H NMR (500 MHz, CDCl_3 , δ): 10.66 (bs, 1H), 7.81 (d, $J = 1.6$ Hz, 1H), 7.65 (d, $J = 8.5$ Hz, 1H), 7.44 (dd, $J_1 = 8.5$ Hz, $J_2 = 1.8$ Hz, 1H), 2.94 (t, $J = 7.3$ Hz, 2H), 2.46 (t, $J = 7.6$ Hz, 2H), 1.73 – 1.66 (m, 4H), 1.37 – 1.30 (m, 2H), 1.04 (t, $J = 7.4$ Hz, 3H), 0.88 (t, $J = 7.3$ Hz, 3H). ^{13}C NMR (125 MHz, CDCl_3 , δ): 171.64, 158.91, 146.43, 132.89, 132.38, 128.68, 122.46, 120.58, 36.91, 36.26, 26.97, 22.54, 22.19, 13.64, 13.38. (+)ESI-HRMS: m/z 309.10813 corresponds to molecular formula $\text{C}_{15}\text{H}_{20}\text{N}_2\text{OS}_2\text{H}^+$ (error, -2.76 ppm). HPLC purity, method A: $t_R = 11.671$, area 97.05%. Method B: $t_R = 13.245$, area 98.01%.

6.2.3.2. *N*-[6-(butylsulfanyl)-1,3-benzothiazol-2-yl]pentanamide (42). Yield 28%. M.p. = 117 °C. IR (ATR): 3144m, 3116m, 3036m, 2958s, 2927s, 2870s, 1694s, 1590s, 1542s, 1443m, 1380m, 1349m, 1306w, 1269s, 1172m, 1099w, 1052w, 976w, 892w, 810m, 769w

cm⁻¹. ¹H NMR (500 MHz, CDCl₃, δ): 10.15 (bs, 1H), 7.80 (d, *J* = 1.6 Hz, 1H), 7.65 (d, *J* = 8.5 Hz, 1H), 7.43 (dd, *J*₁ = 8.5 Hz, *J*₂ = 1.8 Hz, 1H), 2.98 – 2.95 (m, 2H), 2.49 – 2.46 (m, 2H), 1.74 – 1.68 (m, 2H), 1.67 – 1.61 (m, 2H), 1.50 – 1.34 (m, 4H), 0.94 – 0.89 (m, 6H). ¹³C NMR (125 MHz, CDCl₃, δ): 171.61, 158.86, 146.39, 132.87, 132.45, 128.53, 122.31, 120.55, 36.22, 34.53, 31.21, 26.94, 22.16, 21.86, 13.61, 13.59. (+) ESI-HRMS: *m/z* 323.12407 corresponds to molecular formula C₁₆H₂₂N₂OS₂H⁺ (error, -1.73). HPLC purity, method A: *t*_R = 12.200, area 96.72%. Method B: *t*_R = 13.409, area 98.18%.

6.2.3.3. *N*-[6-(butylsulfanyl)-1,3-benzothiazol-2-yl]-2-methoxyacetamide (43). Yield 45%. M.p. = 62 °C. IR (ATR): 3382w, 3207w, 2956m, 2929m, 2871w, 1703m, 1594m, 1537s, 1448m, 1272m, 1196w, 1119m, 994w, 817w, 745w cm⁻¹. ¹H NMR (500 MHz, CDCl₃, δ): 9.86 (bs, 1H), 7.79 – 7.78 (m, 1H), 7.68 (d, *J* = 8.5 Hz, 1H), 7.43 (dd, *J*₁ = 8.5 Hz, *J*₂ = 1.8 Hz, 1H), 4.16 (s, 2H), 3.52 (s, 3H), 2.97 – 2.94 (m, 2H), 1.67 – 1.61 (m, 2H), 1.49 – 1.42 (m, 2H), 0.92 (t, *J* = 7.3 Hz, 3H). ¹³C NMR (125 MHz, CDCl₃, δ): 168.07, 156.52, 146.85, 133.03, 132.65, 128.58, 122.18, 121.26, 71.25, 59.57, 34.55, 31.24, 21.89, 13.61. (+) ESI-HRMS: *m/z* 311.08743 corresponds to molecular formula C₁₄H₁₈N₂O₂S₂H⁺ (error, -2.62 ppm). HPLC purity, method A: *t*_R = 10.999, area 98.02%. Method B: *t*_R = 12.336, area 98.37%.

6.2.3.4. 3-Methoxy-*N*-[6-(propylsulfanyl)-1,3-benzothiazol-2-yl]propanamide (44). Yield 30%. M.p. = 111 °C. IR (ATR): 3270w, 3118m, 3038m, 2962s, 2922s, 2811m, 1704m, 1591s, 1544s, 1447m, 1394m, 1270s, 1174m, 1120m, 1067m, 810m cm⁻¹. ¹H NMR (500 MHz, CDCl₃, δ): 10.26 (bs, 1H), 7.79 (d, *J* = 1.8 Hz, 1H), 7.69 (d, *J* = 8.5 Hz, 1H), 7.43 (dd, *J*₁ = 8.5 Hz, *J*₂ = 1.8 Hz, 1H), 3.76 (t, *J* = 5.5 Hz, 2H), 3.48 (s, 1H), 2.93 (t, *J* = 7.3 Hz, 2H), 2.77 (t, *J* = 5.5 Hz, 2H), 1.71 – 1.64 (m, 2H), 1.03 (t, *J* = 7.3 Hz, 3H). ¹³C NMR (125 MHz, CDCl₃, δ): 169.86, 157.57, 146.97, 133.08, 132.12, 128.67, 122.39, 121.02, 67.67, 59.20, 36.96, 36.90, 22.56, 13.37. (+) ESI-HRMS: *m/z* 311.08741 corresponds to molecular formula C₁₄H₁₈N₂O₂S₂H⁺ (error, -2.67 ppm). HPLC purity, method A: *t*_R = 10.325, area 98.09%. Method B: *t*_R = 11.326, area 99.00%.

6.2.3.5. *N*-[6-(butylsulfanyl)-1,3-benzothiazol-2-yl]-3-methoxypropanamide (45). Yield 32%. M.p. = 99 °C. IR (ATR): 3147s, 3046m, 2953s, 2924s, 2875s, 2814m, 1703s, 1592s, 1536s, 1451m, 1417m, 1395m, 1332m, 1267s, 1160s, 1116s, 1068m, 988w, 960m, 808m, 793m, 757m cm⁻¹. ¹H NMR (500 MHz, CDCl₃, δ): 10.33 (bs, 1H), 7.78 (d, *J* = 1.6 Hz, 1H), 7.69 (d, *J* = 8.5 Hz, 1H), 7.42 (dd, *J*₁ = 8.5 Hz, *J*₂ = 1.8 Hz, 1H), 3.77 – 3.74 (m, 2H), 3.47 (s, 3H), 2.97 – 2.94 (m, 2H), 2.78 – 2.75 (m, 2H), 1.67 – 1.61 (m, 2H), 1.50 – 1.42 (m, 2H), 0.92 (t, *J* = 7.3 Hz, 3H). ¹³C NMR (125 MHz, CDCl₃, δ): 169.88, 157.62, 146.90, 133.07, 132.24, 128.55, 122.24, 121.00, 67.67, 59.18, 36.90, 34.60, 31.26, 21.89, 13.62. (+) ESI-HRMS: *m/z*

325.10332 corresponds to molecular formula $C_{15}H_{20}N_2O_2S_2H^+$ (error, -1.77 ppm). HPLC purity, method A: $t_R = 10.636$, area 96.78%. Method B: $t_R = 12.682$, area 98.30%.

6.2.3.6. 2-Methoxy-N-[6-(propylsulfanyl)-1,3-benzothiazol-2-yl]acetamide (46). Yield 23%. M.p. = 62 °C. IR (ATR): 3170m, 3062m, 2966m, 2938m, 2829w, 1688m, 1590m, 1534s, 1453m, 1273s, 1197m, 1119m, 992w, 809w, 772w, 744w cm^{-1} . 1H NMR (500 MHz, $CDCl_3$, δ): 9.80 (bs, 1H), 7.79 (d, $J = 1.4$ Hz, 1H), 7.69 (d, $J = 8.5$ Hz, 1H), 7.44 (dd, $J_1 = 8.5$ Hz, $J_2 = 1.4$ Hz, 1H), 4.16 (s, 2H), 3.52 (s, 3H), 2.93 (t, $J = 7.2$ Hz, 2H), 1.71 – 1.64 (m, 2H), 1.03 (t, $J = 7.3$ Hz, 3H). ^{13}C NMR (125 MHz, $CDCl_3$, δ): 168.01, 156.40, 146.99, 133.09, 132.48, 128.67, 122.32, 121.32, 71.22, 59.54, 36.90, 22.53, 13.35. (+) ESI-HRMS: m/z 297.07173 corresponds to molecular formula $C_{13}H_{16}N_2O_2S_2H^+$ (error, -2.91 ppm). HPLC purity, method A: $t_R = 10.423$, area 97.81%. Method B: $t_R = 11.602$, area 98.30%.

6.2.4. General procedure F for synthesis of compounds 27 and 38³¹

To a stirring solution of **24** (1 eq) in CH_2Cl_2 , MCPBA (1 eq for **38** and 4 eq for **27**) was added. After stirring (4 h in the dark for compound **38** and 16 h for compound **27**) at room temperature, 10% aqueous $Na_2S_2O_3$ solution was added. The layers were separated, organic layer was washed with saturated aqueous $NaHCO_3$ solution, dried over anhydrous Na_2SO_4 , filtered and evaporated to dryness. The crude product was further purified in a manner provided for each compound.

6.2.4.1. Ethyl [6-(ethanesulfonyl)-1,3-benzothiazol-2-yl]carbamate (27). Yield 55%. M.p. = (257 – 259) °C. IR: 3121m, 3072w, 2979m, 2944m, 2775w, 1721s, 1602m, 1556s, 1450m, 1307s, 1254m, 1150s, 1103w, 1044w, 830w, 786w, 757w, 715w cm^{-1} . 1H NMR (500 MHz, $(CD_3)_2SO$, δ): 12.37 (bs, 1H), 8.58 (d, $J = 0.9$ Hz, 1H), 7.89 – 7.85 (m, 2H), 4.28 (q, $J = 7.1$ Hz, 2H), 3.31 – 3.28 (m, 2H), 1.30 (t, $J = 7.1$ Hz, 3H), 1.12 (t, $J = 7.5$ Hz, 3H). ^{13}C NMR (125 MHz, $CDCl_3$, $(CD_3)_2SO$, δ): 163.77, 153.80, 152.94, 132.42, 132.16, 125.29, 122.37, 120.27, 62.05, 49.76, 14.12, 7.18. (+)ESI-HRMS: m/z 315.04662 corresponds to molecular formula $C_{12}H_{14}N_2O_4S_2H^+$ (error, -0.48 ppm). HPLC purity, method D: $t_R = 4.187$, area 95.46%. Method I: $t_R = 4.662$, area 95.51%.

6.2.4.2. Ethyl [6-(ethanesulfinyl)-1,3-benzothiazol-2-yl]carbamate (38). Yield 28%. M.p. = 195 °C. IR (ATR): 3359m, 3175m, 3056m, 2924s, 2853s, 1713s, 1658m, 1634m, 1602s, 1564s, 1448m, 1366m, 1301s, 1276m, 1250s, 1103m, 1072m, 1044m, 891w, 827w, 794m, 761m, 708w cm^{-1} . 1H NMR (500 MHz, $CDCl_3$, δ): 10.94 (bs, 1H), 8.13 (d, $J = 1.4$ Hz, 1H), 8.02 (d, $J = 8.5$ Hz, 1H), 7.59 (dd, $J_1 = 8.5$ Hz, $J_2 = 1.6$ Hz, 1H), 4.43 (q, $J = 7.1$ Hz, 2H), 3.00 – 2.93 (m, 1H), 2.88 – 2.81 (m, 1H), 1.43 (t, $J = 7.2$ Hz, 3H), 1.23 (t, $J = 7.3$ Hz, 3H). ^{13}C NMR (125 MHz, $CDCl_3$, δ): 163.04, 153.58, 150.90, 138.24, 132.77, 121.84, 121.18, 117.98, 63.26, 50.76, 14.47, 6.14. (+)ESI-HRMS: m/z 299.05162 corresponds to molecular formula

$C_{12}H_{14}N_2O_3S_2H^+$ (error, -0.81 ppm). HPLC purity, method D: $t_R = 4.087$, area 95.52%.

Method I: $t_R = 4.668$, area 95.14%.

6.2.5. General procedure G for synthesis of compounds **39** and **40**³²

To a solution of **28** (1 eq) in methanol, acetonitrile (1.5 eq) and K_2CO_3 (0.7 eq) were added. The mixture is cooled to 0 °C with vigorous stirring and hydrogen-peroxide (1.2 eq for compound **39** and 4 eq for compound **40**) was added dropwise as a solution in methanol over 30 minutes. The reaction was maintained at 0 °C 4 h (for compound **39**) or at room temperature overnight (for compound **40**). After consumption of starting material, the mixture is poured onto brine and extracted with CH_2Cl_2 . Organic layers were dried over anhydrous Na_2SO_4 and evaporated to dryness. The crude product was further purified in a manner provided for each compound.

6.2.5.1. Propyl [6-(propane-1-sulfinyl)-1,3-benzothiazol-2-yl]carbamate (**39**). Yield 26%.

IR (ATR): 3165m, 3127m, 3057m, 2964s, 2933s, 2876s, 2780m, 1724s, 1601s, 1557s, 1449s, 1404m, 1292s, 1274s, 1249s, 1066s, 1032m, 966m, 890m, 829m, 784m, 754m, 708w cm^{-1} . 1H NMR (500 MHz, CD_3OD , δ): 12.21 (bs, N-H), 8.28 – 8.26 (m, 1H), 7.84 – 7.83 (m, 1H), 7.66 – 7.64 (m, 1H), 4.17 (t, $J = 6.6$ Hz, 2H), 2.95 – 2.77 (m, 2H), 1.70 – 1.47 (m, 4H), 0.97 – 0.92 (m, 6H). ^{13}C NMR (125 MHz, CD_3OD , δ): 161.76, 154.08, 151.19, 138.54, 132.39, 121.86, 120.73, 118.13, 67.47, 57.75, 21.63, 15.32, 12.91, 10.09. (+)ESI-HRMS: m/z 327.08293 correspond to molecular formula $C_{14}H_{18}N_2O_3S_2H^+$ (error, -0.72 ppm). HPLC purity, method G: $t_R = 5.365$, area 97.49%. Method H: $t_R = 3.559$, area 96.03%.

6.2.5.2. Propyl [6-(propane-1-sulfonyl)-1,3-benzothiazol-2-yl]carbamate (**40**). Yield 48%.

M.p. = 270 °C. IR (ATR): 3169m, 3125m, 2971s, 2936m, 2880m, 2771w, 1730s, 1598m, 1550s, 1454m, 1405w, 1346w, 1306s, 1279s, 1231s, 1147s, 1103m, 1072m, 942w, 825w, 784m, 757m, 710w cm^{-1} . 1H NMR (500 MHz, CD_3OD , δ): 12.37 (bs, N-H), 8.57 – 8.56 (m, 2H), 7.88 – 7.84 (m, 2H), 4.18 (t, $J = 6.6$ Hz, 2H), 3.30 – 3.26 (m, 2H), 1.72 – 1.66 (m, 2H), 1.60 – 1.53 (m, 2H), 0.96 – 0.89 (m, 6H). ^{13}C NMR (125 MHz, CD_3OD , δ): 164.40, 154.55, 153.40, 133.75, 132.65, 125.91, 123.03, 120.99, 68.09, 57.20, 22.11, 16.76, 12.99, 10.57. (+)ESI-HRMS: m/z 343.07768 corresponds to molecular formula $C_{14}H_{18}N_2O_4S_2H^+$ (error, -1.16 ppm). HPLC purity, method G: $t_R = 5.253$, area 98.21%. Method I: $t_R = 5.480$, area 97.67%.

Full data are given in Supplementary material.

6.3. Biological methods

6.3.1. NCI in vitro antiproliferative screening

Selected compounds were tested initially at a single high dose (10 μM) in the full NCI 60 cell panel through the developmental therapeutics program (DTP) in National Cancer Institute,

Bethesda, MD, USA for evaluating their antiproliferative activity. The compounds which exhibited significant growth inhibition in One-dose Screen, progressed to the full 5-dose assay. The human tumor cell lines of the 60 cells panel were grown in RPMI 1640 medium containing 5% fetal bovine serum and 2 mM L-glutamine. Cells were inoculated into 96 well microtiter plates in 100 μ L at plating densities ranging from 5,000 to 40,000 cells/well depending on the doubling time of individual cell lines. The plates were incubated at 37 °C, 5% CO₂, 95% air and 100% relative humidity for 24 h prior to addition of experimental drugs. Experimental compounds' solutions in DMSO diluted with complete medium containing gentamicin were added to the wells in an appropriate manner resulting in final five drug concentrations, starting at maximum 10⁻⁴M, plus control. Following compound addition, the plates are incubated for an additional 48 h at 37°C, 5% CO₂, 95% air, and 100% relative humidity. After incubation period the cell growth and viability was measured using the sulphorhodamine B (SRB) procedure. There are three dose response parameters calculated for each test compound, growth inhibition of 50% (GI₅₀), total growth inhibition (TGI) and LC₅₀ which represents concentration of compound resulting in a 50% reduction in a measured protein at the end of the treatment as compared to that at the beginning. Values are calculated if the level of activity is reached.

6.3.2. MTT assay

Cell lines used in this study were obtained from the American Type Culture Collection (Rockville, MD) unless specified otherwise. Human breast adenocarcinoma cells (MCF-7), human melanoma cells (A375) and a single human lung fibroblast cell line (MRC-5) were maintained as monolayer culture in nutrient medium, A375 and MRC-5 cells in the Roswell Park Memorial Institute (RPMI) 1640 medium, while MCF-7 cells in the Dulbecco's Modified Eagle's Medium (DMEM). Human myelogenous leukemia cells (K562) were maintained in RPMI as cell suspension. Powdered RPMI 1640 medium, and DMEM modified medium, were purchased from Sigma Chemicals Co, USA. Nutrient medium RPMI 1640 was prepared in sterile deionized water, supplemented with penicillin (192 U/mL), streptomycin (200 μ g/mL), 4-(2-hydroxyethyl) piperazine-1-ethanesulfonic acid (HEPES) (25 mM), L-glutamine (3 mM) and 10% of heat-inactivated fetal calf serum, FCS (pH 7.2). Nutrient medium DMEM modified was prepared in sterile deionized water, supplemented with penicillin (192 U/mL), streptomycin (200 μ g/ mL) and 10% of heat-inactivated FCS. The cells were grown at 37 °C in 5% CO₂ and humidified air atmosphere, by twice weekly subculture. Human embryonal teratocarcinoma cell line (NT2/D1; kind gift of Prof. Paul Andrews, University of Sheffield, UK) was grown in DMEM- high glucose (4500 mg/L glucose) supplemented with 10% fetal bovine serum (FBS), glutamine (2 mM), penicillin (100 U/mL) and streptomycin (100 μ g/mL), all purchased from Invitrogen™, NY,

USA, at 37 °C in 10% CO₂ as described.⁵⁹ The cytotoxic activity of benzothiazole derivatives against MCF-7, A375, K562, NT2/D1 and MRC-5 cell line was assessed using the MTT assay.^{60,61} After treatment with compounds in 96-well plates, 20 µL of MTT solution (3-(4,5-dimethylthiazol-2-yl)-2, 5-diphenyl tetrazolium bromide, Sigma-Aldrich, St. Louis, USA) was added to each well. Samples were incubated for a further 4 h, followed by the addition of 100 µL of 10% SDS. Absorbance was measured the next day. Cell survival was calculated as an absorbance (A570 nm) ratio between treated and control cells multiplied by 100. IC₅₀ was defined as the concentration of the agent that inhibited cell survival by 50% compared to the vehicle control.

6.3.3. NCI toxicity determination in vivo

Acute toxicity in a nontumored female athymic nude mice was assessed following standard procedure.⁶² A single mouse was given a single intraperitoneal (IP) injection of 400 mg/kg; a second mouse received a dose of 200 mg/kg and a third mouse received a single dose of 100 mg/kg. Dose volumes were 1 µL/1 gm body weight. The standard vehicle used was 10% DMSO in saline/0.05% Tween 80. The mice were observed for a period of 2 weeks. The mice are allowed *ad libitum* feed and water. They were sacrificed if they lost more than 20% of their body weight or if there were other signs of significant toxicity. If all three mice were sacrificed, then the next three lower dose levels were tested in a similar way. The process was repeated until a tolerated dose was determined.

6.3.4. Flow-cytometric analysis of cell cycle phase distribution

Briefly, 2x10⁵ cells/Petri dish (dimensions 60 × 15 mm, NUNC) were treated with investigated compounds as indicated. After collection, cells were fixed with ethanol and stained with propidium iodide, PI (Sigma-Aldrich, St. Louis, USA). Cell cycle phase distribution was analyzed by FACS Calibur Becton Dickinson flow cytometer using Cell Quest computer software (BD Biosciences, USA).

6.3.5. Flow cytometric analysis of cyclin B1 expression

Cells stained for FACS analysis were treated as described above. For intracellular cyclin staining the following antibodies were used: FITC-conjugated mouse anti-human cyclin B1 (BD Pharmingen, San Diego, CA, USA), and IgG2a isotype controls (BD Pharmingen, San Diego, CA, USA). Briefly, cells were incubated with antibodies overnight at 4 °C, and washed twice with PBS containing 1% BSA. Cell pellets were resuspended in PBS/PI/DNase-free RNase A and incubated in dark at room temperature for 30 min before acquisition. Samples were analyzed on a FACS-Calibur cytometer using Cell Quest software (BD Biosciences, USA).

6.3.6. Apoptotic assay

Apoptotic rates were assessed with flow cytometry using the Annexin V–fluorescein isothiocyanate/propidium iodide kit (BD Pharmingen, San Diego, CA, USA). Samples were prepared according to manufacturer's instructions. Flow cytometry analysis was performed using a FACS-Calibur cytometer using Cell Quest computer software (BD Biosciences, USA).

6.3.7. Quantification of mitochondrial transmembrane potential

Mitochondrial transmembrane potential ($\Delta\Psi_m$) was measured using a cationic fluorochrome Rhodamine 123 (Rh123, Sigma-Aldrich, St. Louis, USA) as described by Yan et al.³⁴ Briefly, 1×10^6 cells resuspended in 200 μ L of phosphate buffered saline were stained with Rh123 (2.5 μ g/mL) for 30 min at 37 °C. After washing, samples were analyzed by flow cytometry using Cell Quest software (BD Biosciences, USA).

6.3.8. Flow cytometric analysis of apoptotic markers

Cells stained for FACS analysis were treated as described above. For detection of apoptotic cells the following antibodies was used: mouse anti-Bax (BD Pharmingen, San Diego, CA, USA), FITC-conjugated monoclonal Bcl-2 antibody (BD Pharmingen, San Diego, CA, USA). Briefly, cells were incubated with antibodies for 30 min at room temperature and washed twice with PBS containing 1% BSA. Cell pellets were resuspended in PBS and analyzed on a FACS-Calibur cytometer using Cell Quest software (BD Biosciences, USA).

6.3.9. Intracellular staining

For intracellular staining the following antibodies were used: mouse anti-p53 antibody (dilution 1:100, Dako, Glostrup, Denmark) and mouse anti-p73 (5 μ g/mL, Merck Millipore, Darmstadt, Germany). Briefly, cells (5×10^5 cells/flask) were allowed to adhere for 24 h in standard conditions, and then treated as described above (MTT assay). After the stimulation period, cells were fixed immediately by adding pre-warmed Cytofix Buffer for 10 to 12 min at 37°C, and washed twice with PBS containing 1% BSA. After permeabilization of the cells using of Perm Buffer for 20 min at room temperature and washing, cells were incubated with antibodies at room temperature for 60 min protected from light, and washed twice with PBS containing 1% BSA. After appropriate incubation, cells were washed three times with PBS containing 1% BSA and incubated with the corresponding FITC-coupled secondary antibodies (dilution 1:100, BD Pharmingen, San Diego, CA, USA). Samples were analyzed on a FACS-Calibur cytometer using Cell Quest software (BD Biosciences, USA).

6.3.10. Measurement of total intracellular reactive oxygen species

Generation of reactive oxygen species (ROS) was measured using a ROS sensitive fluorescent probe, 2',7'-dichlorodihydrofluorescein diacetate (DCFH-DA). This probe can be oxidized to 2',7'-dichlorofluorescein (DCF) by ROS and exhibits increased green fluorescence intensity. Briefly, the cultured cells were treated with investigated substances and the untreated cells

ACCEPTED MANUSCRIPT
were maintained as the control. After incubation period of 24 or 48 h, the cells were harvested, washed twice, resuspended in 10 mM DCFH-DA and incubated at 37 °C for 30 min in the dark. The levels of intracellular ROS were examined with flow cytometry (FACS Calibur, BD Biosciences, USA). The excitation wavelength was 485 nm, and the fluorescence was measured at 530 nm. Data acquisition and analyses were carried out using Cell Quest software (BD Biosciences, USA).

6.3.11. Wound-healing migration assay

Migration of NT2/D1 cells was analyzed by wound-healing assay. NT2/D1 cells were grown to near confluence and wounded by scraping away regions of the monolayer with pipette tip. Cells were washed with Phosphate Buffer Solution (PBS) and treated either with tested compounds or vehicle control (DMSO). Cell migration was monitored 20 h post-wounding using DM IL LED Inverted Microscope (Leica) and photographed with Leica MC170 HD digital camera attached to the microscope. Cells migrated in cell free area were counted and results for treated cells were presented as a percentage of values obtained for vehicle control.

6.3.12. Colony-forming and colony-growing assays

In the colony-forming assay 600 NT2/D1 cells were seeded in 6 cm plates and immediately treated with tested compounds or vehicle control (DMSO). Media was changed every 48 h. Cells were stained with crystal violet solution on the seventh day after plating and counted using an inverted microscope. In the colony-growing assay, 750 cells were seeded in 6 cm plates and grew until colonies reached the size of ~10 cells. At this stage cells were treated with tested compounds or vehicle control (DMSO) and further grew till colonies consisted of ~50 cells. At this point cells were stained with crystal violet and colonies containing more than 15 cells were counted using an inverted microscope.

6.3.13. In vitro cell invasion assay

Untreated and 24 h treated NT2/D1 cells were seeded in serum-free media at density 1×10^5 cells/well in Transwell chambers (8- μ m-pore filters, Thermo Fisher Scientific) coated with Matrigel (1:3 dilution in serum-free media, Corning). Chemoattractant (media supplemented with 10% FCS) were added to lower chamber. After 48 h incubation surface of the upper chamber were wiped with cotton swabs and cells invaded the lower surface were stained with crystal violet. Inserts were then attached on glass slides and cells from five random microscopic fields were counted and photographed with Leica MC170 HD digital camera attached to the microscope.

Acknowledgements

This research was supported by the Ministry of Science and Technological Development of Serbia Grant 172008 (MV, IO, BŠ), Grant 173051 (MM, MS) and Serbian Academy of Sciences and Arts (BŠ, MS).

Conflict of interest statement

The authors declare no conflict of interest.

References

- ¹ World Health Organization, <http://www.who.int/cancer/en/> (accessed 17 January 2017)
- ² Evan, G. I.; Vousden, K. H. *Nature* **2001**, *411*, 342–348.
- ³ Keri, R. S.; Patil, M. R.; Patil, S. A.; Budagupi, S. A comprehensive review in current developments of benzothiazole-based molecules in medicinal chemistry. *Eur. J. Med. Chem.* **2015**, *89*, 207–251.
- ⁴ Chander, S.P.; Alka, S.; Archana, S.; Harish, R.; Pal, P. D. Medicinal significance of benzothiazole scaffold. *J. Enzyme Inhib. Med. Chem.* **2013**, *28*, (2), 240–266.
- ⁵ Singh, M. K.; Tilak, R.; Nath, G.; Awasthi, S. K.; Agarwal, A. Design, synthesis and antimicrobial activity of novel benzothiazole analogs. *Eur. J. Med. Chem.* **2013**, *63*, 635–644.
- ⁶ Choi, S-J.; Par, H. J.; Lee, S. K.; Kim, S. W.; Han, G.; Choo, H-Y. P. Solid phase combinatorial synthesis of benzothiazoles and evaluation of topoisomerase II inhibitory activity. *Bioorg. Med. Chem.* **2006**, *14*, 1229–1235.
- ⁷ Pitta, E.; Geronikaki, A.; Surmava, S.; Eleftheriou, P.; Mehta, V. P.; Van der Eycken, E. V. Synthesis and HIV-1 RT inhibitory action of novel (4/6-substituted benzo[d]thiazol-2-yl)thiazolidin-4-ones. Divergence from the non-competitive inhibition mechanism. *J. Enzyme Inhib. Med. Chem.* **2013**, *28*, 113–122
- ⁸ Huang, L.; Su, T.; Shan, W.; Luo, Z.; Sun, Y.; He, F.; Li, X. Inhibition of cholinesterase activity and amyloid aggregation by berberine-phenyl-benzoheterocyclic and tacrine-phenyl-benzoheterocyclic hybrids. *Bioorg. Med. Chem.* **2012**, *20*, 3038–3048.
- ⁹ Kaur, H.; Kumar, S.; Singh, I.; Saxena, K. K.; Kumar, A. Synthesis, characterization and biological activity of various substituted benzothiazole derivatives. *Dig. J. Nanomater. Biostruct.* **2010**, *5*, 67–76.
- ¹⁰ Scheetz II, M. E.; Carlson, D. G.; Schinitski, M. R. Frentizole, a novel immunosuppressive, and azathioprine: Their comparative effects on host resistance to *Pseudomonas aeruginosa*, *Candida albicans*, Herpes Simplex Virus, and Influenza (Ann Arbor) Virus. *Infect. Immun.* **1977**, *15*, 145–148.
- ¹¹ Jimonet, P.; Audiau, F.; Barreau, M.; Blanchard, J-C.; Boireau, A.; Bour, Y.; Coléno, M-A.; Doble, A.; Doerflinger, G.; Huu, C. D.; Donat, M-H.; Duchesne, J. M.; Ganil, P.; Guérémy, C.; Honoré, E.; Just, B.; Kerphirique, R.; Gontier, S.; Hubert, P.; Laduron, P. M.; Blevet, J. L.; Meunier, M.; Miquet, J-M.; Nemecek, C.; Pasquet, M.; Piot, O.; Pratt, J.; Rataud, J.; Reibaud, M.; Stutzmann, J-M.; Mignani, S. Riluzole Series. Synthesis and in Vivo “Antigliutamate” Activity of 6-Substituted-2-benzothiazolamines and 3-Substituted-2-imino-benzothiazolines. *J. Med. Chem.* **1999**, *42*, 2828–2843.
- ¹² Ongarora, D. S. B.; Gut, J.; Rosenthal, P. J.; Masimirembwa, C. N.; Chibale, K. Benzoheterocyclic amodiaquine analogues with potent antiplasmodial activity: Synthesis and pharmacological evaluation. *Bioorg. Med. Chem. Lett.* **2012**, *22*, 5046–5050.
- ¹³ Ge, J-F.; Zhang, Q-Q.; Lu, J-M.; Kaiser, M.; Wittlin, S.; Brunb, R.; Ihara, M. Synthesis of cyanine dyes and investigation of their in vitro antiprotozoal activities. *Med. Chem. Commun.* **2012**, *3*, 1435–1442.
- ¹⁴ Burger, A.; Sawhey, S.N. Antimalarials. III. Benzothiazole amino alcohols, *J. Med. Chem.* **1968**, *11*, 270–273.
- ¹⁵ Dar, A. A.; Shadab, M.; Khan, S; Ali, N.; Khan, A. T. One-Pot Synthesis and Evaluation of Antileishmanial Activities of Functionalized S-Alkyl/Aryl Benzothiazole-2-carbothioate Scaffold. *J. Org. Chem.*, **2016**, *81*, (8), 3149–3160.
- ¹⁶ Tapia, R.A.; Prieto, Y.; Pautet, F.; Domard, M.; Sarciron, M.; Walchshofer, N.; Fillion, H. Synthesis and antileishmanial activity of indoloquinones containing a fused benzothiazole ring, *Eur. J. Org. Chem.* **2002**, 4005 – 4010.

- ¹⁷ Leong, C-O.; Gaskell, M.; Martin, E.A.; Heydon, R. T.; Farmer, P.B.; Bibby, M.C.; Cooper, P. A.; Double, J. A.; Bradshaw, T. D.; Stevens, M. F. G. Antitumour 2-(4-aminophenyl)benzothiazoles generate DNA adducts in sensitive tumour cells in vitro and in vivo. *Br. J. Cancer*, **2003**, *88*, 470–477.
- ¹⁸ Mohamed, L. W.; Taher, A. T.; Rady, G. S.; Ali, M. M.; Mahmoud, A. E. Synthesis and cytotoxic activity of certain benzothiazole derivatives against human MCF-7 cancer cell line. *Chem. Biol. Drug Des.* **2016**, 1–11.
- ¹⁹ Subba Rao, A.V.; Swapna, K.; Shaik, S. P.; Nayak, V. L.; Reddy, T. S.; Sunkari, S.; Shaik, T. B.; Bagul, C.; Kamal, A. Synthesis and biological evaluation of cis-restricted triazole/tetrazole mimics of combretastatin-benzothiazole hybrids as tubulin polymerization inhibitors and apoptosis inducers. *Bioorg. Med. Chem.* **2017**, *25*, 977–999.
- ²⁰ Ashraf, Md.; Shaik, T. B.; Malik, M. S.; Syed, R.; Mallipeddi, P. L.; Vardhan, M. V. P. S. V.; Kamal, A. Design and synthesis of cis-restricted benzimidazole and benzothiazole mimics of combretastatin A-4 as antimetabolic agents with apoptosis inducing ability. *Bioorg. Med. Chem. Lett.* **2016**, *26*, 4527–4535.
- ²¹ Lei, Q.; Zhang, L.; Xia, Y.; Ye, T.; Yang, F.; Zhu, Y.; Song, X.; Wang, N.; Xu, Y.; Liua, X.; Yu, L. A novel benzothiazole derivative SKLB826 inhibits human hepatocellular carcinoma growth via inducing G2/M phase arrest and apoptosis. *RSC Adv.* **2015**, *5*, 41341–41351
- ²² Kamal, A.; Ashraf, Md.; Vardhan, M. V. P. S. V.; Faazil, S.; Nayak, V. L. Synthesis and anticancer potential of benzothiazole linked phenylpyridopyrimidinones and their diones as mitochondrial apoptotic inducers. *Bioorg. Med. Chem. Lett.* **2014**, *24*, 147–151.
- ²³ Xie, X.; Yana, Y.; Zhu, N.; Liu, G. Benzothiazoles exhibit broad-spectrum antitumor activity: Their potency, structure-activity and structure-metabolism relationships. *Eur. J. Med. Chem.* **2014**, *76*, 67–78.
- ²⁴ Kamal, A.; Faazil, S.; Ramaiah, M. J.; Ashraf, Md.; Balakrishna, M.; Pushpavalli, S.N.C.V.L.; Patel, N.; Pal-Bhadra, M. Synthesis and study of benzothiazole conjugates in the control of cell proliferation by modulating Ras/MEK/ERK-dependent pathway in MCF-7 cells. *Bioorg. Med. Chem. Lett.* **2013**, *23*, 5733–5739.
- ²⁵ Wang, Z.; Shi, X-H.; Wangb, J.; Zhou, T.; Xu, Y-Z.; Huang, T-T.; Li, Y-F.; Zhao, Y-L.; Yang, L.; Yang, S-Y.; Yu, L-T.; Wei, Y-Q. Synthesis, structure-activity relationships and preliminary antitumor evaluation of benzothiazole-2-thiol derivatives as novel apoptosis inducers. *Bioorg. Med. Chem. Lett.* **2011**, *21*, 1097–1101.
- ²⁶ Yoshida, M.; Hayakawa, I.; Hayashi, N.; Agatsuma, T.; Oda, Y.; Tanzawa, F.; Iwasaki, S.; Koyama, K.; Furukawa, H.; Kurakata, S.; Sugano, Y. Synthesis and biological evaluation of benzothiazole derivatives as potent antitumor agents. *Bioorg. Med. Chem. Lett.* **2005**, *15*, 3328–3332.
- ²⁷ Xuejiao, S.; Yong, X.; Ningyu, W.; Lidan, Z.; Xuanhong, S.; Youzhi, X.; Tinghong, Y.; Yaojie, S.; Yongxia, Y.; Luoting, Y. A Novel Benzothiazole Derivative YLT322 Induces Apoptosis via the Mitochondrial Apoptosis Pathway In Vitro with Anti-Tumor Activity in Solid Malignancies. *PLoS One*, 2013, *8*, e63900
- ²⁸ Corbo, F.; Carocci, A.; Armenise, D.; De Laurentis, N.; Laghezza, A.; Loiodice, F.; Ancona, P.; Muraglia, M.; Pagliarulo, V.; Franchini, C.; Catalano, A. Antiproliferative activity evaluation of a series of N-1,3-benzothiazole-2-ylbenzamides as novel apoptosis inducers. *J. Chem.* **2016**, 1–5.
- ²⁹ Duan, Z.; Ranjit, S.; Liu, X. One-Pot Synthesis of Amine-Substituted Aryl Sulfides and Benzo[b]thiophene Derivatives. *Org. Lett.* **2010**, *12* (10), 2430–2433.
- ³⁰ Li, H.; Li, J.; Chen, H.; Zhang, Y.; Huang, D. Synthesis and Crystal Structure of Charge Transfer Complex (CTC) of 2-Aminobenzothiazole with Its Schiff Base. *J. Chem. Crystallogr.* **2011**, *41*, 1844–1849.
- ³¹ Rennison, D.; Conole, D.; Tingle, M. D.; Yang, J.; Eason, C. T.; Brimble, M.A. Synthesis and methemoglobinemia-inducing properties of analogues of para-aminopropiophenone designed as humane rodenticides. *Bioorg. Med. Chem. Lett.* **2013**, *23*, 6629–6635.
- ³² Bulman Page, P. C.; Graham, A. E.; Bethell, D.; Park, K. A Simple and Convenient Method for the Oxidation of Sulphides. *Synth. Commun.* **1993**, *23* (11), 1507–1514.
- ³³ Boyd, M. R.; Paull, K. D. Some practical considerations and applications of the National Cancer Institute in vitro anticancer drug discovery screen. *Drug Develop. Res.* **1995**, *34*, 91–109.
- ³⁴ Yan, M.; Zhu, P.; Liu, H-M.; Zhang, H-T.; Liu, L. Ethanol induced mitochondria injury and permeability transition pore opening: Role of mitochondria in alcoholic liver disease. *World J. Gastroenterol.* **2007**, *13*, 2352–2356.

- ³⁵ Dalla Via, L.; Garsía-Argáez, A. N.; Martínez-Vázquez, M.; Grancara, S.; Martinis, P.; Toninello, A. Mitochondrial Permeability Transition as Target of Anticancer Drugs. *Curr. Pharm. Des.*, **2014**, *20*, 223–244.
- ³⁶ Strober, W. Trypan blue exclusion test of cell viability. *Curr. Protoc. Immunol.*, **1997**, A.3B.1-A.3B.2 doi:10.1002/0471142735.ima03bs21.
- ³⁷ Frisch, S. M.; Sreaton, R. A. Anoikis mechanisms. *Curr. Opin. Cell Biol.* **2001**, *5*, 555–562.
- ³⁸ Guan, X. Cancer metastases: challenges and opportunities. *Acta Pharm. Sin. B*, **2015**, *5*, 402–418.
- ³⁹ Jin, P.; Hardy, S.; Morgan, D. O. Nuclear localization of cyclin B1 controls mitotic entry after DNA damage. *J. Cell Biol.* **1998**, *141*, 875–885.
- ⁴⁰ Woynarowska, B. A.; Woynarowski, J. M. Preferential targeting of apoptosis in tumor versus normal cells. *Biochim. Biophys. Acta*, **2002**, *1587*, 309–317.
- ⁴¹ Ly, J. D.; Grubb, D. R.; Lawen, A. The mitochondrial membrane potential ($\Delta\psi_m$) in apoptosis; an update. *Apoptosis*, **2003**, *8*, 115–128.
- ⁴² Chipuk, J. E.; Green, D. R. Dissecting p53-dependent apoptosis. *Cell Death Differ.* **2006**, *13*, 994–1002.
- ⁴³ Sayan, A. E.; Sayan, B. S.; Gogvadze, V.; Dinsdale, D.; Nyman, U.; Hansen, T. M.; Zhivotovsky, B.; Cohen, G. M.; Knight, R. A.; Melino, G. p73 and caspase-cleaved p73 fragments localize to mitochondria and augment TRAIL-induced apoptosis. *Oncogene*, **2008**, *27*, 4363–4372.
- ⁴⁴ Janicke, R. U. MCF-7 breast carcinoma cells do not express caspase-3. *Breast Cancer Res. Treat.* **2009**, *117*, 219–221.
- ⁴⁵ Burdon, R. H. Superoxide and hydrogen peroxide in relation to mammalian cell proliferation. *Free Radic. Biol. Med.*, **1995**, *18*, 775–794.
- ⁴⁶ Sullivan, L. B.; Chandel, N. S. Mitochondrial reactive oxygen species and cancer. *Cancer Metab.* **2014**, *2*, 1–17.
- ⁴⁷ Yadav, N. K.; Saini, K. S.; Hossain, Z.; Omer, A.; Sharma, C.; Gayen, J. R.; Singh, P.; Arya, K. R.; Singh, R. K. Saraca indica bark extract shows in vitro antioxidant, antibreast cancer activity and does not exhibit toxicological effects. *Oxid. Med. Cell. Longev.* **2015**, 1–15.
- ⁴⁸ Meredith, J. E. Jr.; Fazeli, B.; Schwartz, M. A. The extracellular matrix as a cell survival factor. *Mol. Biol. Cell.* **1993**, *4*, 953–961.
- ⁴⁹ Frisch, S.M.; Francis, H. J. Disruption of epithelial cell-matrix interactions induces apoptosis. *Cell Biol.* **1994** *124*, 619–626.
- ⁵⁰ Syrigos, K. N.; Karayiannakis, A. J. Adhesion molecules as targets for the treatment of neoplastic diseases. *Curr. Pharm. Des.* **2006**, *12*, 2849–2861.
- ⁵¹ Nakamura, T.; Miki, T. Recent strategy for the management of advanced testicular cancer. *Int. J. Urol.* **2010**, *17*, 148–157.
- ⁵² Pabla, N.; Dong, Z. Cisplatin nephrotoxicity: mechanisms and renoprotective strategies. *Kidney Int.* **2008**, *73*, 994–1007.
- ⁵³ Sheth, S. Current and emerging therapies for patients with advanced non-small-cell lung cancer. *Am. J. Health Syst. Pharm.* **2010**, *67*, 9–14.
- ⁵⁴ Garcion, E.; Naveilhan, P.; Berger, F.; Wion, D. Cancer stem cells: beyond Koch's postulates. *Cancer Lett.* **2009**, *278*, 3–8.
- ⁵⁵ Paget, S. The distribution of secondary growths in cancer of the breast. *Lancet*, **1889**, *133*, 571–573.
- ⁵⁶ Szarynska, M.; Olejniczak, A.; Kobiela, J.; Spsychalski, P.; Kmiec, Z. Therapeutic strategies against cancer stem cells in human colorectal cancer. *Oncol. Lett.* **2017**, *14*, 7653–7668.
- ⁵⁷ Pelicano, H.; Carney, D.; Huang, P. ROS stress in cancer cells and therapeutic implications. *Drug Resist. Updates*, **2004**, *7*, 97–110.
- ⁵⁸ Tietze, L. F.; Güntner, C.; Gericke, K. M.; Schuberth, I.; Bunkoczi, G. A Diels–Alder reaction for the total synthesis of the novel antibiotic antitumor agent mensacarcin. *Eur. J. Org. Chem.*, **2005**, 2459–2467.
- ⁵⁹ Andrews, P.W.; Retinoic acid induces neuronal differentiation of a cloned human embryonal carcinoma cell line in vitro. *Dev. Biol.*, **1984**, *103*, 285–293.
- ⁶⁰ Mosmann, T.; Rapid colorimetric assay for cellular growth and survival: Application to proliferation and cytotoxicity assays. *J. Immunol. Methods*, **1983**, *65*, 55–63.
- ⁶¹ Ohno, M.; Abe, T.; Rapid colorimetric assay for the quantification of leukemia inhibitory factor (LIF) and interleukin-6 (IL-6). *J. Immunol. Methods*, **1991**, *145*, 199–203.
- ⁶² https://dtp.cancer.gov/organization/btb/acute_toxicity.htm (accessed 21 May 2018).

- New antiproliferative benzothiazole carbamates and amides are synthesized
- Benzothiazoles induce apoptosis and G2/M arrest along with ROS reduction in MCF-7 cells
- Detached NT2/D1 cells that underwent apoptosis point to anoikis
- Benzothiazole derivatives strongly inhibit migration and invasiveness of NT2/D1 cells
- The most potent compounds show no toxicity in vitro and in vivo

ACCEPTED MANUSCRIPT